Molecular Vision 2011; 17:63-69 <http://www.molvis.org/molvis/v17/a9>
Received 13 October 2010 | Accepted 4 January 2011 | Published 8 January 2011

Tissue factor expression in human pterygium

Ryo Ando,[1] Satoru Kase,[1] Tsutomu Ohashi,[2] Zhenyu Dong,[1] Junichi Fukuhara,[1] Atsuhiro Kanda,[1] Miyuki Murata,[1,3] Kousuke Noda,[1] Nobuyoshi Kitaichi,[3,4] Susumu Ishida[1,3]

[1]Laboratory of Ocular Cell Biology and Visual Science, Department of Ophthalmology, Hokkaido University Graduate School of Medicine, Sapporo, Japan; [2]Ohashi Eye Center, Sapporo, Japan; [3]Department of Ocular Inflammation and Immunology, Hokkaido University Graduate School of Medicine, Sapporo, Japan; [4]Department of Ophthalmology, Health Sciences University of Hokkaido, Sapporo, Japan

Purpose: A pterygium shows tumor-like characteristics, such as proliferation, invasion, and epithelial–mesenchymal transition (EMT). Previous reports suggest that tissue factor (TF) expression is closely related to the EMT of tumor cells, and subsequent tumor development. In this study, we analyzed the expression and immunolocalization of TF in pterygial and normal conjunctival tissues of humans.

Methods: Eight pterygia and three normal bulbar conjunctivas, surgically removed, were used in this study. Formalin-fixed, paraffin-embedded tissues were submitted for immunohistochemical analysis with anti-TF antibody. Double staining immunohistochemistry was performed to assess TF and alpha-smooth muscle actin (α-SMA) or epidermal growth factor receptor (EGFR) expression in the pterygia.

Results: Immunoreactivity for TF was detected in all pterygial tissues examined. TF immunoreactivity was localized in the cytoplasm of basal, suprabasal, and superficial epithelial cells. The number of TF-immunopositive cells in pterygial epithelial cells was significantly higher than in normal conjunctival epithelial cells ($p<0.001$). TF immunoreactivity was detected in α-SMA-positive or -negative pterygial epithelial cells. EGFR immunoreactivity was detected in pterygial epithelium, which was colocalized with TF.

Conclusions: These results suggest that TF plays a potential role in the pathogenesis and development of a pterygium, and that TF expression might be involved through EMT-dependent and -independent pathways.

A pterygium represents an epithelial and fibrovascular configuration on the ocular surface adjoining the conjunctiva. The pterygium invades the cornea forming a wing-like shape, causing visual loss. Pathologically, a pterygium is a proliferative, invasive, and highly vascularized tissue [1]. Furthermore, there are transformed cells in pterygial tissue, which is one of the characteristics of a tumor phenotype [2]. Kase et al. [3,4] demonstrated that proliferation activity is high in the pterygial epithelium compared to that in the normal conjunctiva.

The phenomenon of epithelial cells changing their phenotype to fibroblastic cells after morphogenic pressure from injured tissue is called epithelial–mesenchymal transition (EMT) [5,6]. To develop highly invasive characteristics, epithelial tumor cells change their morphology and function, whereby they transiently acquire markers of mesenchymal differentiation (e.g., alpha-smooth muscle actin (α-SMA)), and lose some of their epithelial features (e.g., E-cadherin) [7]. Moreover, blockade of E-cadherin in cultured cancer cells similarly leads to changes in cell shape reminiscent of EMT, and this transition gave rise to cells with a highly metastatic phenotype. It has been demonstrated that E-cadherin immunoreactivity is involved in α-SMA-positive pterygial epithelial cells [4,8], suggesting that EMT plays a key role in the pathogenesis of pterygium.

Tissue factor (TF) is a transmembrane protein that interacts with coagulation factor VIIa, whereby it initiates blood coagulation. This interaction also triggers intracellular signals, which are primarily mediated by G protein–coupled protease-activated receptors in concert with adhesion molecules and several other factors [9]. TF is regulated by oncogenic and differentiation pathways and it functions in tumor initiation, tumor growth, angiogenesis, and metastasis [9-11]. Indeed, it has been demonstrated that epithelial tumor cells, expressing high levels of TF regulated by the differentiation pathway, have mesenchymal characteristics [9]. These results suggest that TF expression is closely related to the EMT of tumor cells, and subsequent tumor development.

The aim of this study was to analyze the expression and immunolocalization of TF in pterygial and conjunctival tissues in humans.

METHODS

Preparation of human tissues: Eight patients with primary nasal pterygia who underwent surgical excision were enrolled in this study. Normal bulbar conjunctival tissues were obtained from three patients during cataract surgery. The

Correspondence to: Satoru Kase, Department of Ophthalmology, Hokkaido University Graduate School of Medicine, N15 W7, Kita-ku, Sapporo, 060-8638 Japan; Phone: +81-11-706-5944; FAX: 81-11-706-5948; email: kaseron@med.hokudai.ac.jp

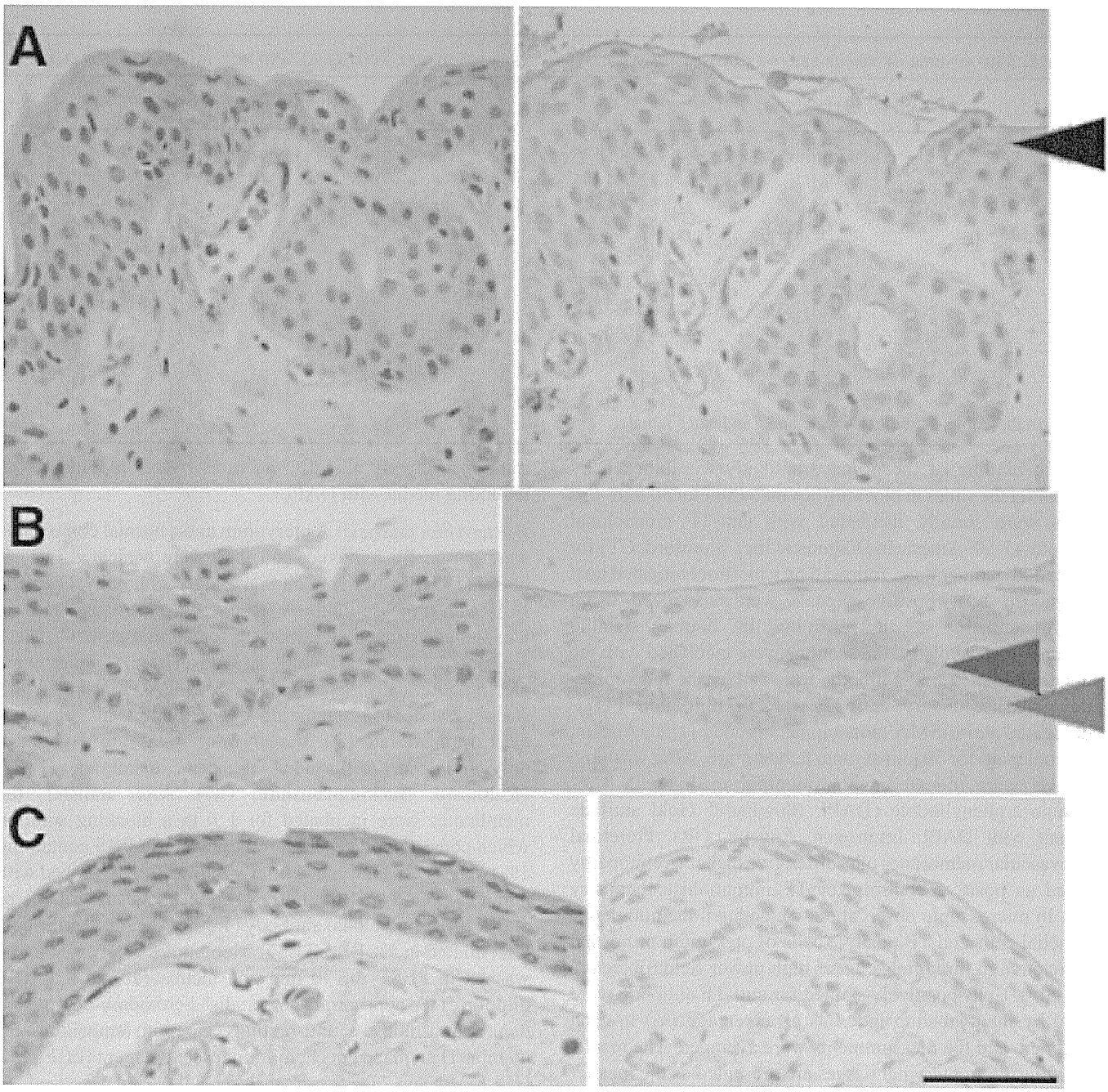

Figure 1. Immunohistochemistry for tissue factor (TF) in a human pterygium and normal conjunctiva. Left panels are H&E staining and right panels are TF immunoreactivity in two representative cases of a pterygium. TF is expressed in the cytoplasm of basal (**B**; red arrow head), suprabasal (**B**; blue arrow head), and superficial cells (**A**; black arrow head). In the normal conjunctiva, however, immunoreactivity for TF is not detected (**C**). The scale bar represents 50 μm.

tissues were then fixed in 4% paraformaldehyde. After fixation, slides were washed in phosphate-buffered saline and processed for paraffin sectioning. Informed consent was obtained according to the Declaration of Helsinki. All human experiments conformed to the requirements of ethics committee in Hokkaido University Graduate School of Medicine.

Immunohistochemistry: Dewaxed paraffin sections were immunostained using the alkaline phosphatase complex method. Formalin-fixed, paraffin-embedded serial tissue sections were cut at a 4 μm thickness and endogenous peroxidase activity was inhibited by immersing the slides in 3% hydrogen peroxide in methanol for 10 min. As a pretreatment, microwave-based antigen retrieval was performed in phosphate-buffered saline (PBS). Then, non-

TABLE 1. THE NUMBER OF TISSUE FACTOR (TF)-IMMUNOPOSITIVE CELLS IN PTERYGIAL EPITHELIAL AND NORMAL CONJUNCTIVAL CELLS.

Pterygia			Normal conjunctivas		
Age	**Gender**	**TF**	**Age**	**Gender**	**TF**
72	M	12.7%	54	M	0%
83	M	54.8%	80	M	0%
75	F	47.7%	82	M	0%
72	M	69.8%			
71	M	69.1%			
68	M	84.3%			
77	M	45.0%			
69	M	54.9%			
	Mean	54.8%		Mean	0%

In the Table, M indicates male and F indicates female.

specific binding of the primary antibody was blocked by incubating the slides in blocking bovine serum for 30 min. The slides were serially incubated with anti-TF monoclonal antibody (1:50; American Diagnostic Inc., Stamford, CT) for 2 h at room temperature, followed by a biotin-conjugated goat anti-mouse IgG. Positive signals were visualized using diaminobendizine as a substrate. In double staining immunohistochemistry, the sections were incubated with the above-mentioned first antibody, followed by the rhodamine-conjugated secondary antibody for 30 min, and FITC-conjugated anti-α-SMA monoclonal antibody (1:50; Abcam, Tokyo, Japan) for 30 min at room temperature. After washing, sections were mounted with mounting media with 4',6-diamino-2-phenylindole (DAPI; SlowFade® Gold antifade reagent with DAPI; Invitrogen, Eugene, OR). Preretinal fibrovascular membranes of proliferative diabetic retinopathy served as positive controls for TF immunohistochemistry [12]. In microscopic observation, we counted the number of epithelial cells and TF-positive cells of pterygium or normal conjunctiva in three fields under high power field (objective lens 40×). Cells positively stained for anti-TF antibody were noted by their labeling index as a percentage (%) in each specimen, and the measurements were averaged. The results regarding TF in pterygial tissues are presented as the mean.

To investigate the hypothesized co-localization of TF and EGFR in pterygium tissues, double staining immunohistochemistry was performed using mouse monoclonal antibody against human TF (1:50; Abcam) and anti-rabbit epidermal growth factor receptor (EGFR) polyclonal antibody (1:100 dilution; Santa Cruz Biotech, Santa Cruz, CA) as the primary antibody. Binding of the primary antibody was localized with the Alexa Fluor® 488 goat anti-mouse antibody (1:100 dilution; Invitrogen, Carlsbad, CA) and Alexa Fluor® 546 goat anti-rabbit secondary antibody (1:200 dilution; Invitrogen) for 30 min, respectively. Finally, sections were mounted with mounting media with DAPI.

Western blot analysis: A pterygium and a normal conjunctiva were surgically removed, and then were sonicated in lysis buffer (1× RIPA buffer; Cell Signaling Technology, Danvers, MA) with protease inhibitor (Roche, Basel, Switzerland) on ice, and centrifuged at 1,3850× g for 20 min at 4 °C. These are stored in −80 °C until assayed. These samples were electrophoretically separated on SDS–PAGE using a 4% stacking and 10% separating gels. Proteins in gels were electro-transferred (80 V, 90 min, 4 °C) to Hybond-P polyvinylidene difluoride transfer membranes (GE Healthcare, Buckinghamshire, UK). After transfer, the membranes were incubated for 1 h in a blocking solution which consisted of 1% skim milk powder in PBS containing 1% tween (PBST), washed briefly in PBST, then probed with anti-TF monoclonal antibody (1:500; above described) or anti-α-SMA polyclonal antibody (1:500; Abcam, Cambridge, UK) diluted in 5% BSA/TBST. Membranes were extensively washed in PBST for 30 min and incubated with a 1:1000 dilution of the appropriate horseradish peroxidase-conjugated donkey anti-mouse or anti-rabbit IgG at room temperature for 60 min. Then placed in chemiluminescent reagent (ECL plus, GE healthcare, Buckinghamshire, UK) and exposed to luminescent image analyzer (Fujifilm, Tokyo, Japan).

Statistical analysis: Student's t-test was used for statistical comparison of the number of TF-immunopositive epithelial cells between pterygium and normal control groups. Differences between the means were considered significant when the probability values were <0.05.

RESULTS

Morphologically, pterygial epithelium consisted of multilayer nuclei showing squamous metaplasia (Figure 1A). Table 1 summarizes the immunohistochemical results of TF in pterygial epithelium. Immunoreactivity for TF was detected

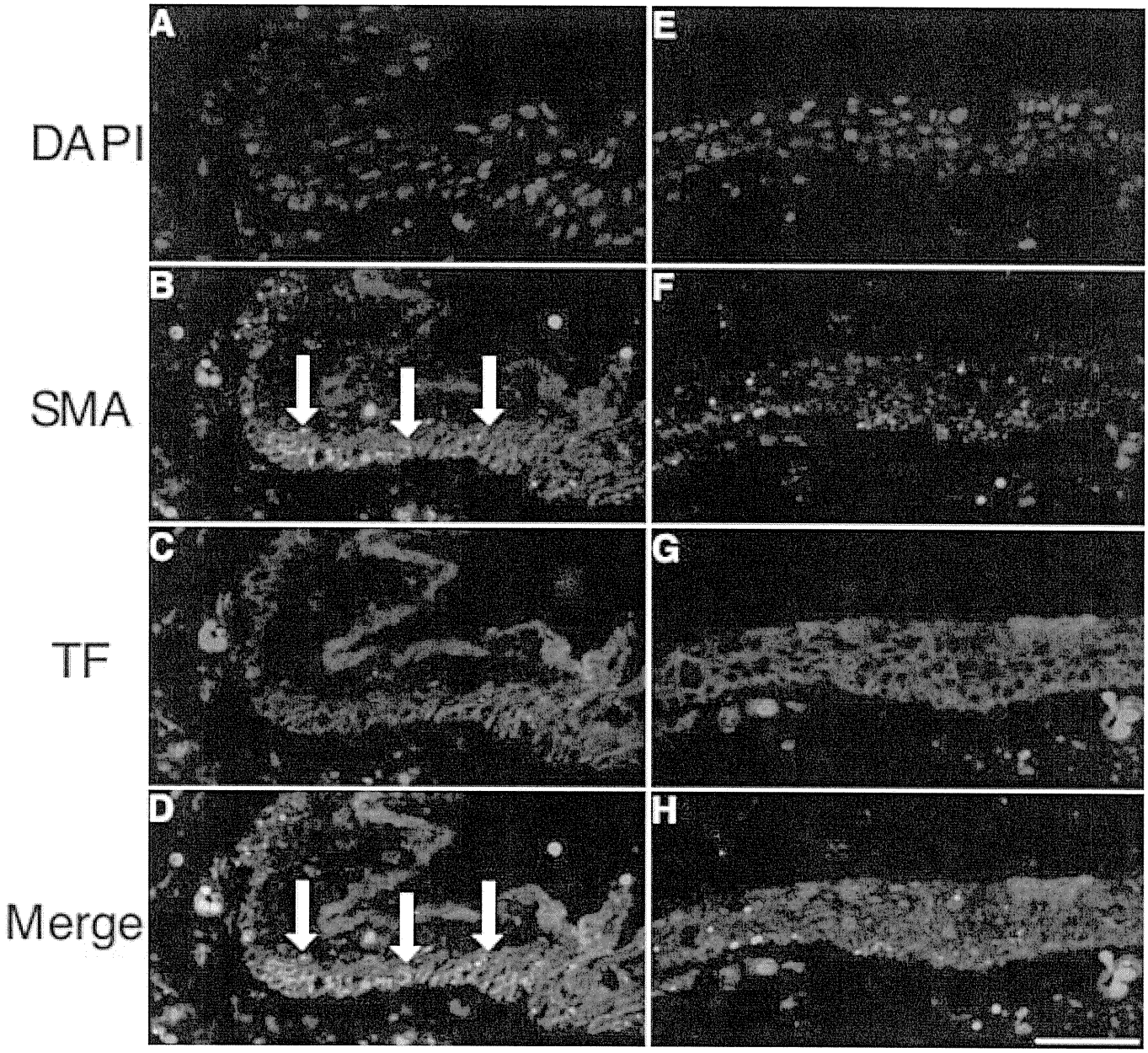

Figure 2. Double staining immunohistochemistry was performed for TF (red) and α-SMA (green) in pterygial tissue. **A-D**: α-SMA immunoreactivity is colocalized with TF-positive areas in pterygial epithelial cells (**D**, arrows). **E-H**: TF immunoreactivity is detected in the other part of epithelial cells negative for α-SMA. The scale bar represents 50 μm.

in all pterygial tissues examined. TF immunoreactivity was localized in the cytoplasm of basal, suprabasal, and superficial epithelial cells, and in subepithelial stroma along with epithelium (Figure 1A,B). In the normal conjunctival epithelium, however, immunoreactivity for TF was not detected (Figure 1C). Microvascular endothelial cells showed a weak immunoreaction for TF in both normal conjunctiva and pterygium. The number of TF-immunopositive cells was significantly higher in pterygial epithelial cells than in normal cells ($p<0.001$; Table 1).

Double staining immunohistochemistry involving pterygial tissues was performed for TF and α-SMA expression. α-SMA was expressed in several epithelial cells (Figure 2B,F), where TF immunoreactivity was colocalized (Figure 2C,G). TF immunoreactivity was also detected in α-SMA-negative epithelial cells (Figure 2E-H).

To check the expression of TF and α-SMA by other methods in human pterygium and normal conjunctiva, western blot analysis was performed using anti-TF and α-SMA antibodies. TF and α-SMA protein expression was

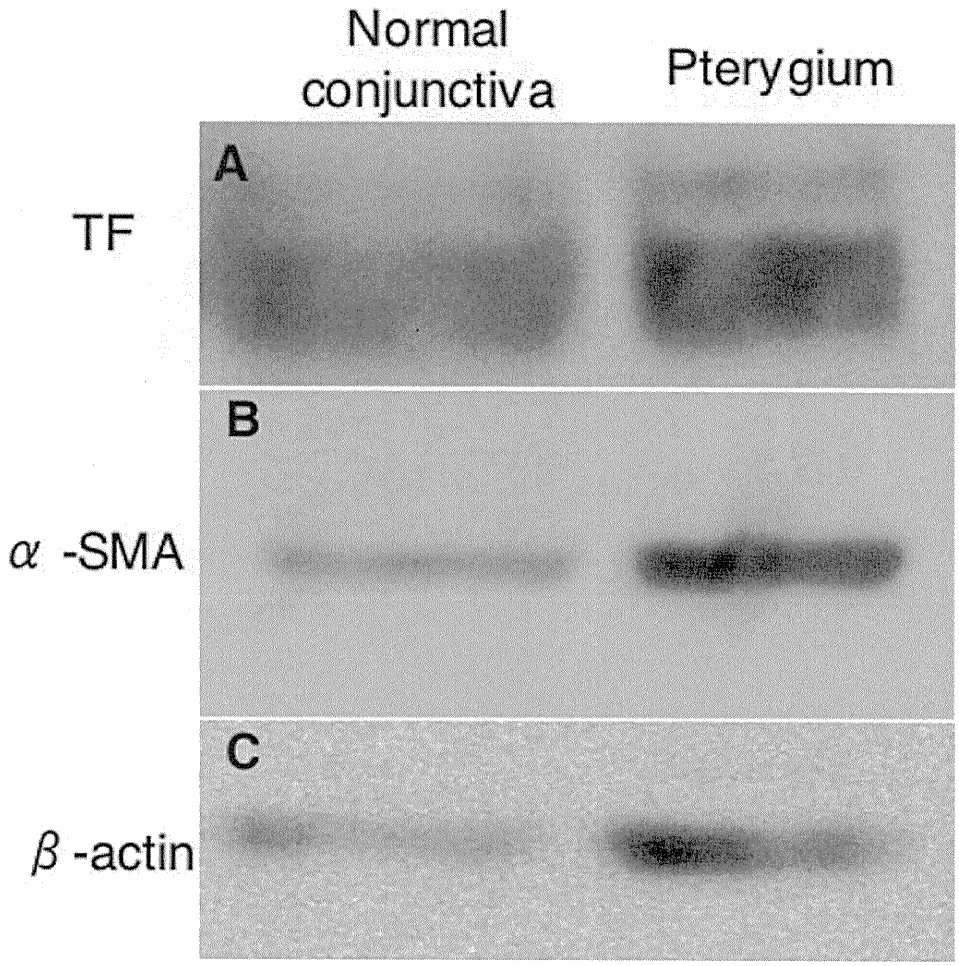

Figure 3. Western blot analysis using anti-TF and α-SMA antibodies. TF (**A**) and α-SMA (**B**) protein expression is clearly detected in both pterygium and normal conjunctival tissue.

clearly detected in both total proteins extracted from pterygium and normal conjunctival tissues (Figure 3).

Double staining immunohistochemistry for TF and EGFR was also performed in pterygial tissue. EGFR immunoreactivity was observed in pterygial epithelial cells, which was colocalized with TF in preferentially basal cells (Figure 4).

DISCUSSION

Pterygium has common biologic features with epithelial tumor, as is proliferative tissue and presence of EMT cells [8]. It has been demonstrated that TF functions in tumor initiation, tumor growth, angiogenesis, and metastasis [9-11]. Therefore, we supposed that TF might play a key role in the pathogenesis of pterygium; however, TF expression has yet to be determined in human pterygium. In this study, we demonstrated that TF protein was expressed in pterygial tissues using immunohistochemistry and western blot. Moreover, TF was mainly immunolocalized in pterygial epithelial cells. As shown in Table 1, the number of TF-positive cells was more than half of that of pterygial epithelial cells. In contrast, TF was not expressed in normal conjunctival epithelium. Microvascular endothelial cells showed a weak immunoreaction for TF in both the normal conjunctiva and pterygium, which was not significant. The result showing a significantly higher expression of TF in pterygial epithelium than the normal conjunctiva suggests that TF plays a role in the pathogenesis and development of a pterygium.

EMT is a major factor in pterygium progression [8]. In this study, protein expression of α-SMA, a classic sign of EMT, was observed in several pterygial epithelial cells, where TF immunoreactivity was colocalized on double staining immunohistochemistry. These results indicate that epithelial cells changing to the mesenchymal phenotype expressed TF. In tumor cells, Milsom et al. [9] demonstrated that E-cadherin modulated TF expression, and this could be alleviated by EMT-like changes. These results suggest that TF expression might be controlled by EMT in pterygium as well.

On the other hand, we found that pterygial epithelial cells, showing a negative results for α-SMA, also expressed TF. This suggests that the expression of TF is regulated not only by E-cadherin and EMT, but also by other TF-related molecules such as epidermal growth factor-receptor (EGFR). We and other colleagues previously demonstrated that E-

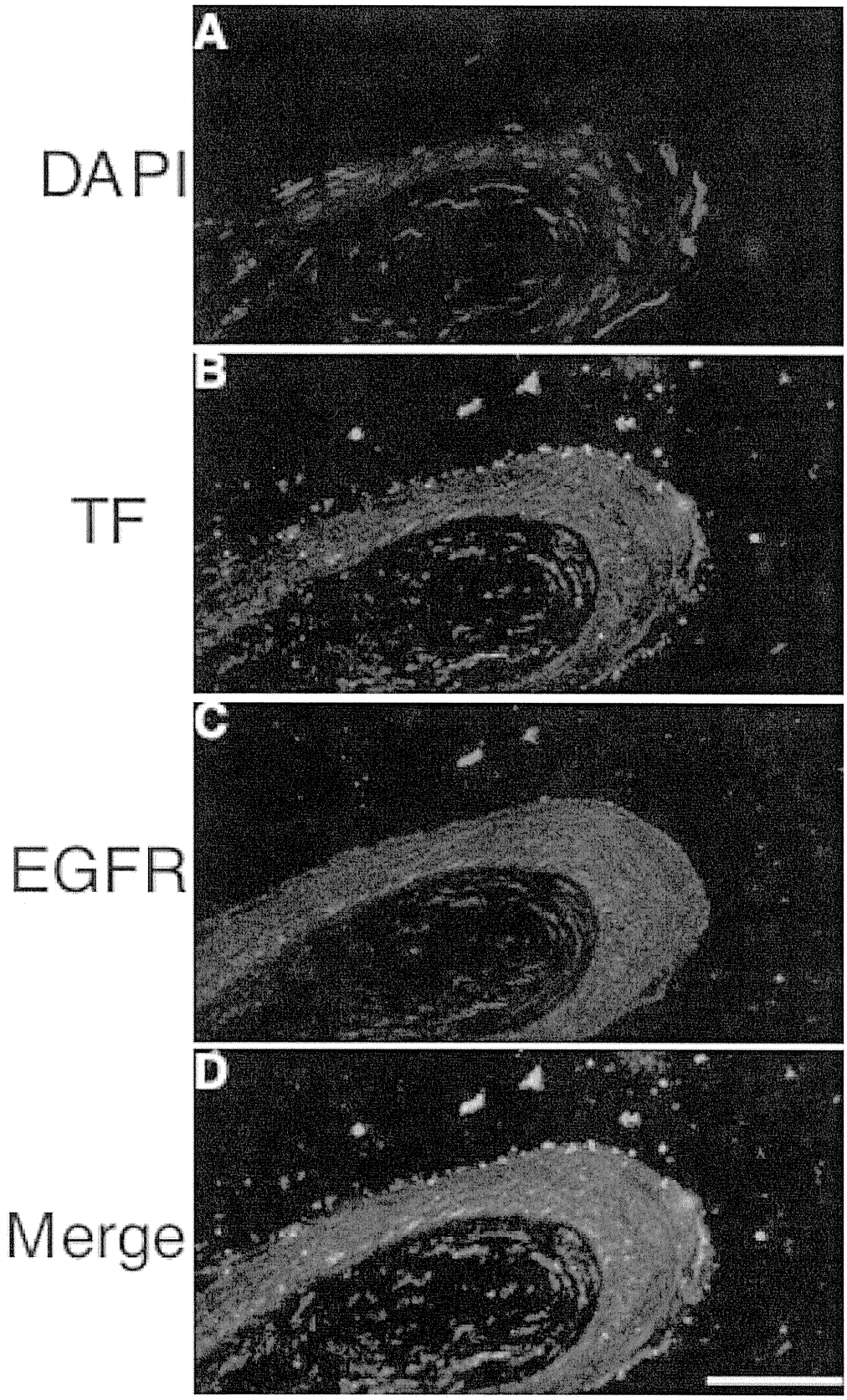

Figure 4. Double staining immunohistochemistry was performed for TF (green) and EGFR (red) in pterygial tissue. Nuclear staining and TF immunoreactivity are shown in **A** and **B**, respectively. **C**, **D**: EGFR immunoreactivity was observed broadly in pterygial epithelial cells. The scale bar represents 50 μm.

cadherin and EGFR immunoreactivity were shown by pterygial epithelial cells [4,8,13], and we immunohistochemically showed colocalization with TF and EGFR. In human squamous cell carcinoma, the activation of EGFR stimulates TF expression, which is modulated by E-cadherin in vitro, and an E-cadherin-neutralizing antibody led to the upregulation of TF expression [9]. Indeed, this induction of TF was completely inhibited by an EGFR inhibitor [9]. These findings suggest that EGFR signaling pathway may also play an important role in the regulation of TF expression.

It has been demonstrated that subsequent EMT and the activation of TF signaling can induce angiogenesis, tumor growth, and invasion [9]. In fact, invasion to the cornea and angiogenesis are characteristics in the pathobiology of a pterygium. Further investigations of the TF signaling pathway in the pterygium are necessary to clarify TF-mediated pterygial progression. Since targeting TF has been considered to be of therapeutic significance in tumor initiation [9], TF may be a therapeutic molecular target to treat pterygia.

ACKNOWLEDGMENTS

This study was supported by the Research foundation of the Japan Society for the Promotion of Science, by a grant for Research on Sensory and Communicative Disorders from The Ministry of Health, Labour, and Welfare, and by grants-in-aid for Scientific Research from The Ministry of Education, Culture, Sports, Science, and Technology (MEXT).

REFERENCES

1. Gebhardt M, Mentlein R, Schaudig U, Pufe T, Recker K, Nolle B, Al-Samir K, Geerling G, Paulsen FP. Differential expression of vascular endothelial growth factor implies the limbal origin of pterygia. Ophthalmology 2005; 112:1023-30. [PMID: 15885787]
2. Spandidos DA, Sourvinos G, Kiaris H, Tsamparlakis J. Microsatellite instability and loss of heterozygosity in human pterygia. Br J Ophthalmol 1997; 81:493-6. [PMID: 9274415]
3. Kase S, Takahashi S, Sato I, Nakanishi K, Yoshida K, Ohno S. Expression of p27(KIP1) and cyclin D1, and cell proliferation in human pterygium. Br J Ophthalmol 2007; 91:958-61. [PMID: 17179165]
4. Kase S, Osaki M, Sato I, Takahashi S, Nakanishi K, Yoshida K, Ito H, Ohno S. Immunolocalisation of E-cadherin and beta-catenin in human pterygium. Br J Ophthalmol 2007; 91:1209-12. [PMID: 17360734]
5. Postlethwaite AE, Shigemitsu H, Kanangat S. Cellular origins of fibroblasts: possible implications for organ fibrosis in systemic sclerosis. Curr Opin Rheumatol 2004; 16:733-8. [PMID: 15577612]
6. Zeisberg M, Kalluri R. The role of epithelial-to-mesenchymal transition in renal fibrosis. J Mol Med 2004; 82:175-81. [PMID: 14752606]
7. Thiery JP, Sleeman JP. Complex networks orchestrate epithelial-mesenchymal transitions. Nat Rev Mol Cell Biol 2006; 7:131-42. [PMID: 16493418]
8. Kato N, Shimmura S, Kawakita T, Miyashita H, Ogawa Y, Yoshida S, Higa K, Okano H, Tsubota K. Beta-catenin activation and epithelial-mesenchymal transition in the pathogenesis of pterygium. Invest Ophthalmol Vis Sci 2007; 48:1511-7. [PMID: 17389479]
9. Milsom CC, Yu JL, Mackman N, Micallef J, Anderson GM, Guha A, Rak JW. Tissue factor regulation by epidermal growth factor receptor and epithelial-to-mesenchymal transitions: effect on tumor initiation and angiogenesis. Cancer Res 2008; 68:10068-76. [PMID: 19074872]
10. Rickles FR. Mechanisms of cancer-induced thrombosis in cancer. Pathophysiol Haemost Thromb 2006; 35:103-10. [PMID: 16855354]
11. Ruf W, Fischer EG, Huang HY, Miyagi Y, Ott I, Riewald M, Mueller BM. Diverse functions of protease receptor tissue factor in inflammation and metastasis. Immunol Res 2000; 21:289-92. [PMID: 10852129]
12. Sakamoto T, Ito S, Yoshikawa H, Hata Y, Ishibashi T, Sueishi K, Inomata H. Tissue factor increases in the aqueous humor of proliferative diabetic retinopathy. Graefes Arch Clin Exp Ophthalmol 2001; 239:865-71. [PMID: 11789868]
13. Di Girolamo N, Coroneo M, Wakefield D. Epidermal growth factor receptor signaling is partially responsible for the increased matrix metalloproteinase-1 expression in ocular epithelial cells after UVB radiation. Am J Pathol 2005; 167:489-503. [PMID: 16049334]

Articles are provided courtesy of Emory University and the Zhongshan Ophthalmic Center, Sun Yat-sen University, P.R. China. The print version of this article was created on 6 January 2011. This reflects all typographical corrections and errata to the article through that date. Details of any changes may be found in the online version of the article.

Bone marrow transplantation restores epidermal basement membrane protein expression and rescues epidermolysis bullosa model mice

Yasuyuki Fujita[a], Riichiro Abe[a,1], Daisuke Inokuma[a], Mikako Sasaki[a], Daichi Hoshina[a], Ken Natsuga[a], Wataru Nishie[a], James R. McMillan[a], Hideki Nakamura[a], Tadamichi Shimizu[b], Masashi Akiyama[a], Daisuke Sawamura[c], and Hiroshi Shimizu[a,1]

[a]Department of Dermatology, Hokkaido University Graduate School of Medicine, Sapporo 060-8638, Japan; [b]Department of Dermatology, Toyama University Graduate School of Medicine and Pharmaceutical Sciences, Toyama 930-0194, Japan; and [c]Department of Dermatology, Hirosaki University Graduate School of Medicine, Hirosaki 036-8562, Japan

Edited* by Douglas Lowy, National Institutes of Health, Bethesda, MD, and approved June 24, 2010 (received for review January 4, 2010)

Attempts to treat congenital protein deficiencies using bone marrow-derived cells have been reported. These efforts have been based on the concepts of stem cell plasticity. However, it is considered more difficult to restore structural proteins than to restore secretory enzymes. This study aims to clarify whether bone marrow transplantation (BMT) treatment can rescue epidermolysis bullosa (EB) caused by defects in keratinocyte structural proteins. BMT treatment of adult collagen XVII (Col17) knockout mice induced donor-derived keratinocytes and Col17 expression associated with the recovery of hemidesmosomal structure and better skin manifestations, as well improving the survival rate. Both hematopoietic and mesenchymal stem cells have the potential to produce Col17 in the BMT treatment model. Furthermore, human cord blood CD34$^+$ cells also differentiated into keratinocytes and expressed human skin component proteins in transplanted immunocompromised (NOD/SCID/γ_c^{null}) mice. The current conventional BMT techniques have significant potential as a systemic therapeutic approach for the treatment of human EB.

hematopoietic stem cells | type XVII collagen

Bone marrow-derived cells, including hematopoietic stem cells and mesenchymal stem cells, have been reported to play a significant role in the recovery of various impaired organs (1–8). Although some papers have reported that "transdifferentiation" of circulating hematopoietic stem cells is an extremely rare event (9), previous reports have shown that expression of systemic enzymes and certain secreted factors can be recovered after bone marrow transplantation (BMT) (10).

Epidermolysis bullosa (EB) comprises a group of genodermatoses, which are caused by mutations in one of the genes encoding anchor proteins that stabilize the basement membrane zone (BMZ) of the skin and mucous membranes (11). Collagen XVII (COL17) is a transmembrane component of hemidesmosomal adhesion structures anchoring cells to the BMZ. *COL17* is the gene underlying non-Herlitz junctional EB in humans, a disorder that causes severe skin fragility, hair loss, growth retardation, and enamel hypoplasia (11). There is no effective treatment for EB other than palliative care. Gene-treated cultured autografting, reported by Mavilio et al. (12), is a promising therapeutic approach for junctional EB. However, its effects are limited to the area of application, in addition to the ethical and safety problems of using viruses for gene correction, even if the recent development of lentiviral vectors with favorable safety might be able to avoid the risks of gene augmentation with traditional retroviral constructs (13). Therefore, systemic and ethically safer therapies would be preferable.

Previous work reported that cells of human or murine origin do home to the skin, such as in graft-versus-host disease in humans (14) and epithelial progenitors in murine bone marrow (15). Our group reported that donor-derived keratinocytes could be identified at wound sites in a BMT model (16). This suggests that BMT techniques have the potential to provide functional keratinocytes over the entire skin surface. The current study investigates whether BM-derived cells can differentiate into donor-derived keratinocytes and subsequently produce detectable COL17 protein after BMT, with the ultimate goal of improving the clinical phenotype and contributing to long-term survival in our model mice.

Results

Donor BM-Derived Cells Express Col17 Protein in the BMZ in Recipient Mouse Skin. To investigate whether BM-derived keratinocytes can produce skin component proteins, we transplanted BM-derived cells of C57BL/6 mice expressing *human COL17* (*hCOL17*) driven by the keratin 14 promoter ($COL17^{m+/+,h+}$) into wild-type C57BL/6 mice in the first set of experiments. Detection of hCOL17 protein in the epithelized recipient skin would indicate that donor BM-derived cells had differentiated into keratinocytes. Immunohistochemical analysis revealed hCOL17 protein expression in the BMZ within the wounded area for four out of the eight BMT-treated C57BL/6 mice (Fig. 1*A*). RT-PCR analysis also showed evidence of *hCOL17* mRNA expression in five out of the eight treated mice (Fig. 1*B*).

We subsequently performed another BMT experiment: BM-derived cells from GFP$^+$ Tg mice were transplanted into COL17-humanized ($COL17^{m-/-,h+}$) mice (Fig. S1) (17). In this experimental pattern, BM-derived cells that differentiated into keratinocytes in the host mice were found to have the potential to produce mCol17 protein. BM-derived nonhematopoietic cells expressing GFP$^+$ CD45$^-$ were sparsely observed, accounting for $1.83 \pm 0.82\%$ ($n = 5$) of the basal layer cells (Fig. 1*C*). Aggregated GFP$^+$ cytokeratin$^+$ cells were also found in the basal cell layer (Fig. 1*D*). Epithelized skin areas in this experiment demonstrated mCol17 protein expression, although unwounded areas of the transplanted $COL17^{m-/-,h+}$ mice failed to express that protein (Fig. 1*E*). This mCol17 expression lasted at least 9 mo after wound formation in two out of the three investigated mice (Fig. S2). RT-PCR analysis also revealed the expression of *mCol17* mRNA in epithelized skin from four of the five transplanted mice, indicating that the BM-derived epidermal cells were able to express active *mCol17* (Fig. 1*F*).

Author contributions: Y.F., R.A., D.I., W.N., T.S., M.A., D.S., and H.S. designed research; Y.F., D.I., M.S., D.H., K.N., W.N., J.R.M., H.N., and D.S. performed research; K.N. and W.N. contributed new reagents/analytic tools; and Y.F., R.A., M.S., J.R.M., M.A., and H.S. analyzed data; and Y.F. and R.A. wrote the paper.

The authors declare no conflict of interest.

*This Direct Submission article had a prearranged editor.

[1]To whom correspondence may be addressed. E-mail: aberi@med.hokudai.ac.jp or shimizu@med.hokudai.ac.jp.

This article contains supporting information online at www.pnas.org/lookup/suppl/doi:10.1073/pnas.1000044107/-/DCSupplemental.

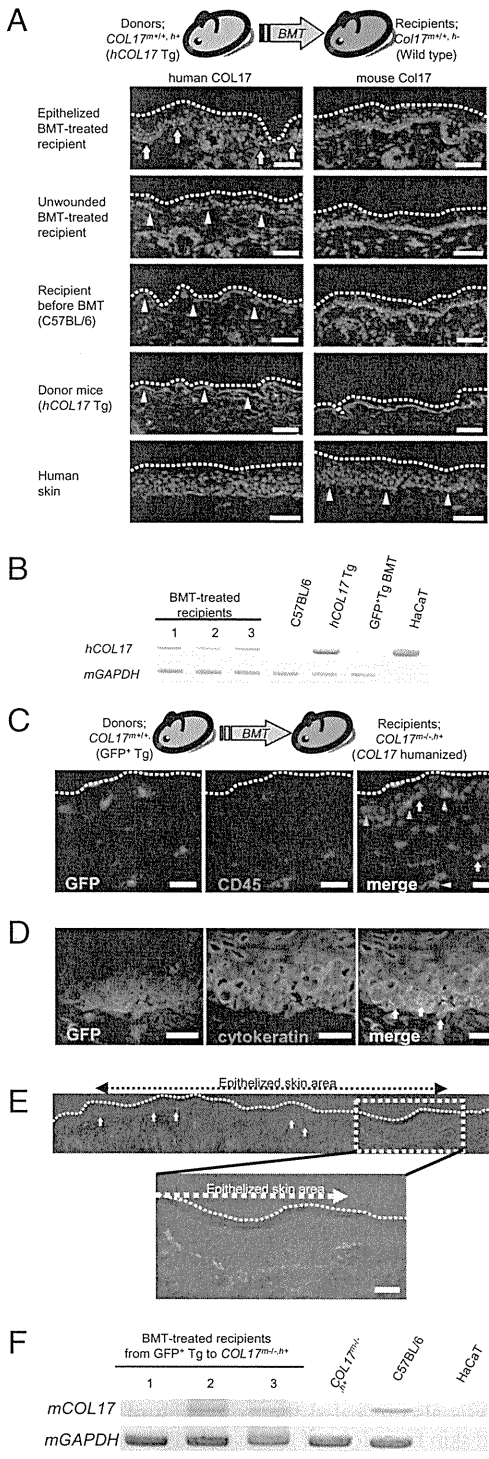

Fig. 1. BMT-induced donor cell-derived COL17 in the epithelized skin tissue. (*A*) The donor-derived hCOL17 expression is observed in the epithelized skin areas of BMT-treated C57BL/6 recipients (yellow arrows). Green: mCol17 (KT4.2) or hCOL17 (D20); red: nuclei; broken lines: skin surface; arrowheads: BMZ. (Scale bars: 50 μm.) (*B*) Representative RT-PCR analysis for *hCOL17* expression reveals positive bands in BMT-treated C57BL/6 recipients. All RNA samples were extracted from full-thickness skin biopsies, except for HaCaT from cultured cells. (*C*) Immunohistochemical analysis of the BMT-treated $COL17^{m-/-,\ h+}$ skin tissue demonstrates donor-derived GFP^+ $CD45^+$ blood cells (yellow arrowheads) and recipient-derived GFP^- $CD45^+$ cells (yellow arrow). Donor-derived GFP^+ $CD45^-$ (green arrowheads) cells are sporadically noted in the epidermis. (Scale bars: 20 μm.) (*D*) Aggregated donor-derived GFP^+ cells in the basal cell layer are noted, some of which also express cytokeratin (white arrows). These cells are thought to be donor-derived keratinocytes. (Scale bars: 20 μm.) (*E*) The skin of the recipients shows sporadic, linear deposition of mCol17 (arrows). The deposition is limited to the epithelized skin area with acanthosis. (*Upper*) The entire consolidated image. (*Lower*) Higher magnification. (Scale bars: 50 μm.) (*F*) RT-PCR analysis shows the recovery of *mCol17* mRNA in two out of three representative mice (lanes 2 and 3).

BM-Derived Cells Supply Deficient Col17 Protein in the Col17 Knockout EB Model Mice. Our group recently established non-Herlitz junctional EB model mice ($COL17^{m-/-}$) as a result of homozygous ablation of the Col17 gene (17). Unlike EB model mice reported by other researchers, our model has allowed us to obtain adult $COL17^{m-/-}$ mice that can be used for various therapeutic strategies (Fig. S3). We speculated that mCol17 protein would be reintroduced by administering BM-derived cells from BMT treatments into $COL17^{m-/-}$ EB model mice. We transplanted BM cells of the GFP^+ Tg mice into the $COL17^{m-/-}$ mice. All of the mice obtained hematopoietic chimeras (710. ± 4.0%, $n = 21$). Immunohistochemical analysis revealed sporadic GFP^+ cells in the basal cell layer of the epidermis, accounting for 1.08 ± 0.39% of the basal cells ($n = 11$). GFP^+ $CD45^-$ cells including $cytokeratin^+$ epidermal keratinocytes were also found (0.26% ± 0.08% of basal cells) (Fig. 2*A* and Fig. S4). Linear deposition of mCol17 along the BMZ, and GFP^+ cells above the mCol17 staining were observed, accounting for 14.7 ± 3.0% ($n = 11$) of the epithelized area (Fig. 2*B*). Also, a 180-kDa mCol17 protein was detected in Western blotting (Fig. 2*C*). One out of three mice showed positive mCol17 immunohistochemically in unwounded skin from the back (Fig. S5*A*). Eight out of nine BMT-treated mice showed positive *mCol17* mRNA in the epithelized skin tissues. Compared with unwounded skin, epithelized areas of skin tended to show *mCol17* mRNA expression more frequently (Fig. S5*B*). We also performed RT-PCR analysis on the epithelized areas of BMT-treated $COL17^{m-/-}$ mice from the epidermis and the dermis by detaching each side enzymatically; this revealed positivity only on the epidermal side (Fig. 2*D*). Next, we sorted GFP^+ cells from the single-cell suspension of epithelized epidermal cells. A portion of the suspended epidermal cells showed GFP (1.24 ± 0.12%, $n = 4$; Fig. S6), and mRNA expression specific to epidermal keratinocytes was detected from the extract of the GFP^+ epidermal cells. These cells also expressed *mCol17* mRNA in three out of the four investigated mice (Fig. 2*E*). To rule out the possibility that cell fusion was occurring between BM cells and original keratinocytes in the $COL17^{m-/-}$ mice, we performed FISH analysis in a sex-mismatched BMT model. Several fused cells with XXXY chromosomes in the same nucleus were found in the deep dermis of the epithelized skin (Fig. 2*F*). Conversely, no fused cells were found in the epidermis of the samples we investigated, whereas 50 of 1,793 basal cells (2.79%) showed donor-derived XY chromosomes. To investigate the restoration of COL17 expression and its effect on restoring normal BMZ structure, we performed electron microscopic analysis. In the BMT-treated $COL17^{m-/-}$ mice, a portion of the basal cells had mature hemidesmosomes (Fig. 2*G*). The average thickness of outer plaques of hemidesmosomes was 79.7 ± 3.2 nm in the wild-type mice, 45.1 ± 1.4 nm in the untreated $COL17^{m-/-}$ mice, and 61.1 ± 1.9 nm in the BMT-treated $COL17^{m-/-}$ mice ($P < 0.01$). To exclude the nonspecific effects of bone marrow infusion, a mixture of $lineage^+$ differentiated GFP^+ BM cells and $lineage^-$ $COL17^{m-/-}$ BM cells was transplanted into the $COL17^{m-/-}$ mice. No Col17 expression of mRNA and protein were detected in the epithelized skin ($n = 3$).

Col17 Knockout Mice Exhibit Less Severe Clinical Manifestations and Better Survival Prognosis After BMT than Untreated Mice. To investigate the change in vulnerability to friction in skin that resulted from the restoration of Col17, we rubbed the back of each mouse (18). The BMT-treated mice ($n = 6$) significantly showed formation of smaller erosions compared with the untreated mice ($n = 4$) (Fig. 3*A*). Although our $COL17^{m-/-}$ mice survived longer than previously reported EB models, only 12.5% of the mice survived to 1 mo, approximately half of which died within the following 3 mo (17). Surprisingly, 16 out of the 20 transplanted $COL17^{m-/-}$ mice survived to 100 d after BMT (transplanted on d 35 after birth), whereas only 7 out of the 17 untreated $COL17^{m-/-}$ mice survived to

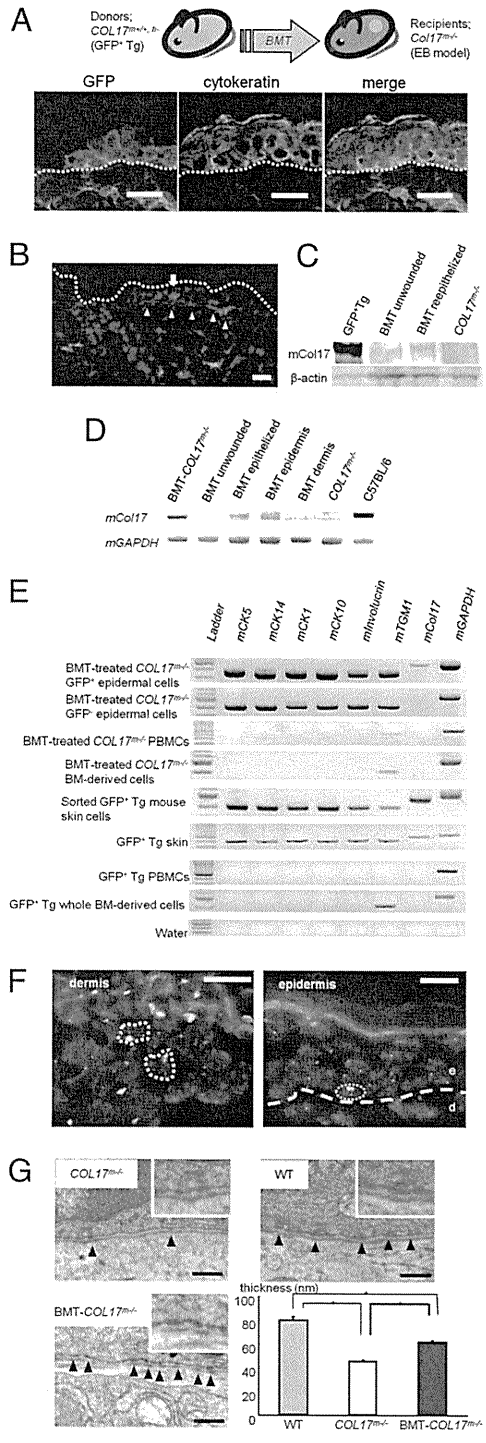

Fig. 2. BMT treatments induce functional mCol17 in *COL17*$^{m-/-}$ junctional EB model mice. (*A*) In the epithelized skin tissue of BMT-treated mice, a cluster of GFP$^+$ cytokeratin$^+$ basal cells is observed. Green: GFP; blue: nuclei; broken lines: skin surface. (Scale bars: 10 μm.) (*B*) Sporadic GFP$^+$ cells (green) are shown in the epithelized skin of the recipients (arrow). Furthermore, linear staining of mCol17 is detected in the BMZ (red, KT4.2, arrowheads). (Scale bars: 20 μm.) (*C*) Western blotting analysis reveals the expression of mCol17 in the epithelized area of the BMT-treated *COL17*$^{m-/-}$ mouse (lane 3), and a weak band is seen in unwounded skin of a BMT-treated *COL17*$^{m-/-}$ mouse (lane 2). β-actin: loading control. (*D*) The expression of *mCol17* is detected only in the epithelized skin and not in the unwounded skin area. Also, the expression is limited to the epidermis side of the epithelized skin. (*E*) The sorted GFP$^+$ single epidermal cells of BMT-treated *COL17*$^{m-/-}$ mice express various keratinocyte-specific mRNAs as well as *mCol17*. Sorted GFP$^-$ cells express these mRNAs, other than that of mCol17. (*F*) No fused cells are apparent in the epidermis, although donor-derived XY cells are sparsely shown. Sporadic fused cells with XXXY chromosomes are observed in the deep dermis. Dashed circles indicate the border of the nucleus. e: epidermis; d: dermis. (Scale bars: 10 μm.) (*G*) The epithelized skin of *COL17*$^{m-/-}$ mice has hypoplastic hemidesmosomes with thin, poorly formed inner/outer plaques (arrowheads). In BMT-treated *COL17*$^{m-/-}$ mice, hemidesmosomes with mature plaques are seen. (Scale bars: 500 nm.) $^*P < 0.01$.

d 135 after birth. The survival outcomes were 73.7% for the transplanted group and 27.5% for the untreated group at d 200 after BMT (Fig. 3*B*). The BMT technique brought significant therapeutic benefits to the *COL17*$^{m-/-}$ EB model mice.

The untreated adult *COL17*$^{m-/-}$ EB model mice showed spontaneous erosions, ulcers, nail deformity, hair loss, and hair graying similar to those seen in human junctional EB patients lacking *COL17* (17). The erosions were especially severe in the genital regions (Fig. 3*C*). The BMT-treated *COL17*$^{m-/-}$ mice showed improvements to clinical manifestations, with fewer spontaneous erosions than for the untreated *COL17*$^{m-/-}$ mice and BMT-control *COL17*$^{m-/-}$ mice (*COL17*$^{m-/-}$ mice as donors). The improvements were particularly marked in the genital regions (Fig. S7).

Both Hematopoietic and Mesenchymal Stem Cells Contribute to the Expression of Col17. Because BM cells consist of various differentiated hematopoietic cells and stem cells, there is the question of which type of BM-derived stem cells produced the Col17 and caused clinical improvement in the *COL17*$^{m-/-}$ EB model mice. We obtained hematopoietic stem cells (HSCs) and multipotent mesenchymal stromal cells (MSCs) from GFP$^+$ Tg mice, following transplantation of each type of stem cell into *COL17*$^{m-/-}$ mice with whole *COL17*$^{m-/-}$ BM-derived cells as supporting cells (Fig. 4*A*). Four weeks after BMT, we confirmed partial chimerism (37.0 ± 13.7%, $n = 5$) of GFP in peripheral blood of BMT-treated mice with GFP$^+$ HSCs (HSC-BMT mice), whereas no GFP$^+$ peripheral blood cells were detected in BMT-treated mice with GFP$^+$ MSCs (MSC-BMT mice, $n = 4$) (Fig. S8). Immunohistochemical analysis revealed sparse GFP$^+$ cytokeratin$^+$ keratinocytes in the skin of the HSC- and MSC-BMT mice (Fig. 4*B*). Both HSCs and MSCs were found to have the potential to produce mCol17 as observed immunohistochemically; three out of five HSC-BMT mice and two out of four MSC-BMT mice showed positive mCol17 (Fig. 4*C*). RT-PCR analysis also demonstrated the expression of *mCol17* in both the HSC-BMT model (three out of five mice) and the MSC-BMT model (two out of four mice) (Fig. 4*D*). HSC-BMT mice showed better clinical manifestations than untreated *COL17*$^{m-/-}$ mice, whereas mice of the MSC-BMT model had a tendency to show more severe perianal erosions and hair loss (Fig. 4*E*).

Transplanted Human Cord Blood CD34$^+$ Cells Obtain a Keratinocyte-Like Phenotype and Produce Epidermal Component Proteins. Toward clinical applications of stem cell transplantation therapies in human EB patients, we investigated whether the human hematopoietic stem cells have the ability to supply structural proteins in the BMZ of the skin. A human-to-mouse xenogeneic transplantation model was investigated using NOD/SCID/γ_c^{null} (NOG) mice (19). Using immunohistochemistry, human cells that expressed human leukocyte antigen (HLA)-ABC could be seen, and pancytokeratin-positive cells were sporadically costained (0.39 ± 0.15% of the basal cells, $n = 4$) (Fig. 5*A* and *B*), which indicates that these cells are donor cell-derived keratinocytes. In addition, sparse and intermittent hCOL17 was detected along the BMZ in two of seven treated mice (Fig. 5*C*). RT-PCR analysis surprisingly showed mRNA expression of several components of the normal human BMZ other than *hCOL17* (detected in six of seven treated mice), including *BPAG1* (four of seven), *plectin* (four of seven), *α6 integrin* (five of seven), *laminin β3* (two of seven), and *laminin γ2* (one out of seven) (Fig. 5*D*).

Discussion

Junctional EB is caused by mutations in the genes coding for structural proteins anchoring the skin to the underlying basal

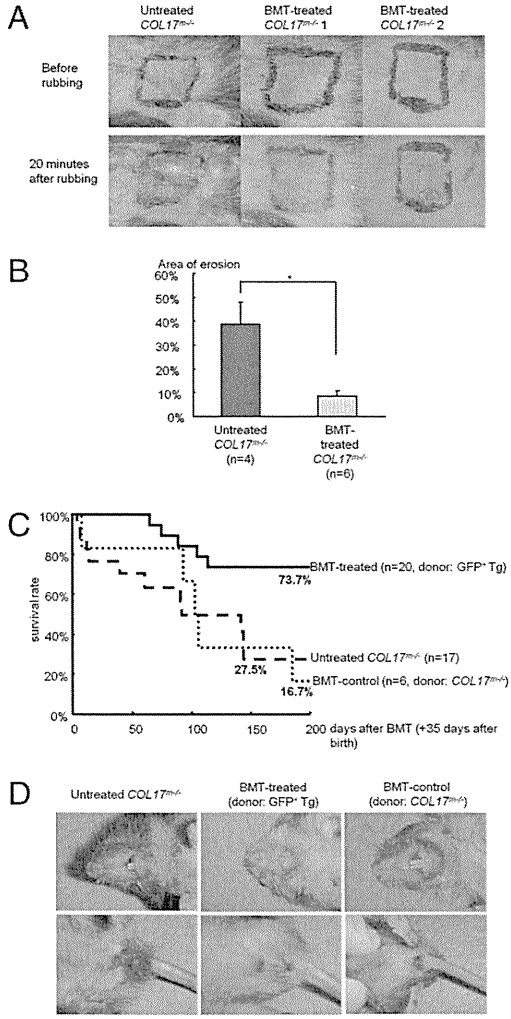

Fig. 3. BMT treatments in $COL17^{m-/-}$ junctional EB model mice change vulnerability to friction in the skin and induce better clinical conditions. (*A*) epithelized areas after erosion formation are investigated by rubber stress test. In untreated $COL17^{m-/-}$ mice, mild mechanical stimulus induces large erosions. Conversely, BMT-treated mice show less severe erosions. $*P < 0.05$. (*B*) The erosion area expressed as a percent of the rubbed area is measured for each group. Resistance of the skin to mechanical stimuli is significantly improved in the BMT-treated $COL17^{m-/-}$ mice. (*C*) Survival curves of BMT-treated and -untreated $COL17^{m-/-}$ mice from d 35 after birth (the day of BMT). $COL17^{m-/-}$ mice treated with BMT from $COL17^{m-/-}$ mice are shown as the BMT control mice; 73.7% of BMT-treated $COL17^{m-/-}$ mice could be expected to live over 200 d after BMT treatment vs. only 27.5% of untreated $COL17^{m-/-}$ mice and 16.7% of BMT control mice. ($P = 0.015$ for BMT-treated vs. untreated mice, $P = 0.021$ for BMT-treated vs. BMT control, and $P = 0.964$ for BMT control vs. untreated.). (*D*) Clinical manifestations at 90 d after BMT treatment (125 d after birth). Untreated $COL17^{m-/-}$ mice show moderate perioral erosions with crusts and anal erosions occurring spontaneously. In contrast, BMT-treated $COL17^{m-/-}$ mice show mild erosions in these areas.

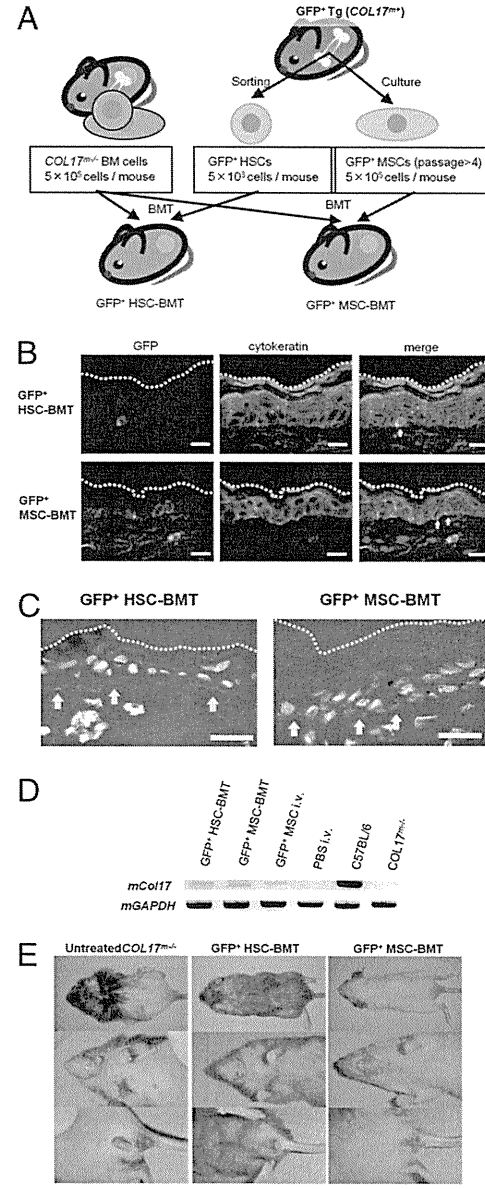

Fig. 4. HSCs and MSCs each have the potential to produce mCol17 in transplanted $COL17^{m-/-}$ mice. (*A*) HSCs and MSCs from GFP^+ Tg mice were sorted or cultured. One or the other type of these stem cells with supporting $COL17^{m-/-}$ whole BM cells were injected into preirradiated $COL17^{m-/-}$ mice. (*B*) Sparse GFP^+ cytokeratin$^+$ cells, shown by white arrows, are detected in the epithelized skin of HSC-BMT model mouse (*Upper*). Also in the MSC-BMT model, GFP^+ cytokeratin$^+$ cells are observed (*Lower*). (Scale bars: 10 μm.) (*C*) Punctate staining of mCol17 is noted, shown as yellow arrows, in the epithelized skin tissue of both HSC- and MSC-BMT model mice. (Scale bars: 20 μm.) (*D*) RT-PCR analysis of the epithelized skin area after full-thickness wounding. Both HSCs (lane 1) and MSCs (lane 2) in the BMT treatment model express positive *mCol17*. Also, single i.v. injection of GFP^+ MSCs (lane 3) induces weak *mCol17* mRNA expression. (*E*) At 90 d after treatment, the HSC-BMT model mice (*Center*) demonstrate better clinical manifestations than the untreated $COL17^{m-/-}$ mice (*Left*), whereas mice of the MSC-BMT models (*Right*) tend to show more severe perianal erosions and hair loss.

lamina and dermis. Recently, various treatments were reported to restore the deficient proteins. These approaches fall mainly into three strategies: gene therapy (20–24), protein therapy (21, 25, 26), and cell therapy. Cell therapies using fibroblasts have been attempted for recessive dystrophic EB (RDEB) model mice and human patients, both of which lack collagen VII. Intradermal fibroblast cell therapy was reported for RDEB model mice (18) and RDEB human patients (27). These approaches may prove to be fundamental treatments for EB. However, their effects are transient and occur only where the genes, proteins, or cells are introduced; they may cause rejection and such gene-correction approaches still raise questions of ethics and safety. Woodley et al. (28) recently reported that i.v. injection of human fibroblasts induces systemic production of human collagen VII in immunodeficient mice; however, major ethical and safety problems remain in human patients.

BMT, an established, widely used medical technique for hematologic malignancies, has recently been attempted for severe hereditary genetic disorders. Hobbs et al. (29) first reported the

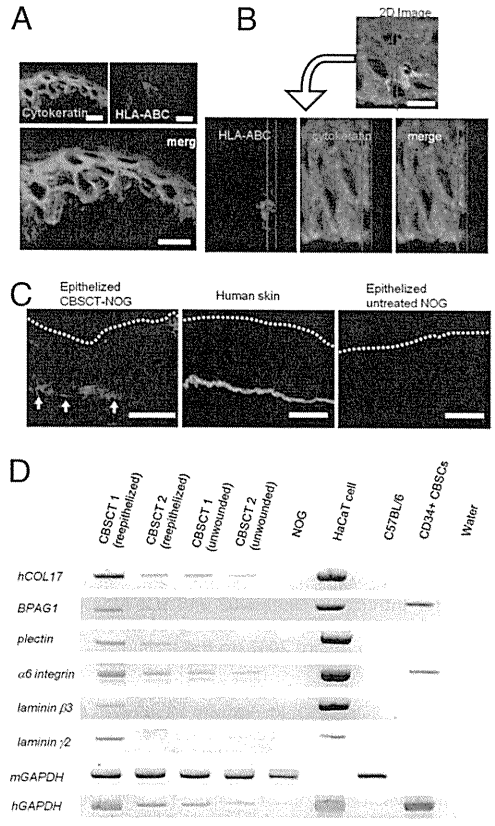

Fig. 5. Human hematopoietic stem cell transplantation induces human epidermal keratinocytes that produce BMZ proteins. (*A*) The epithelized skin samples of treated NOG mice include sporadic cytokeratin$^+$ (red), HLA-ABC$^+$ (blue) cells in the basal cell layer, which indicate human cord blood-derived keratinocytes. (Scale bars: 10 μm.) (*B*) 3D analyses of the immunohistochemical sections prove costaining of keratin (red) and HLA-ABC (green), indicating that these cells are human cord blood-derived keratinocytes and not two distinct overlaid cells. Blue lines: cross-section edges. (Scale bar: 10 μm.) (*C*) Sparse, linear deposition of hCOL17 is noted in the epithelized skin of CBSCT-treated NOG mice (yellow arrows). Green: hCOL17 (D20); red: cytokeratin; (Scale bars: 20 μm.) (*D*) RT-PCR analysis for two transplanted NOG mice, for both unwounded and epithelized skin (CBSCT 1 and CBSCT 2). The expression of several BMZ proteins, *hCOL17, BPAG1, plectin, α6 integrin, laminin β3*, and *laminin γ2* mRNA is demonstrated. Unwounded skin shows faint expression of *hCOL17* and *α6 integrin*.

efficacy of BMT for treatment of Hurler's syndrome. Later hematopoietic stem cell transplantation proved effective in other mucopolysaccharidoses (30–33). More recently, Sampaolesi et al. (34) reported on the potential of stem cell therapy for the treatment of Duchene muscular dystrophy. These experiments indicate that stem cell therapies including BMT are promising candidates for several congenital genetic disorders. BMT techniques have three advantages over previous cell therapies: (*i*) systemic and long-lasting effects can be expected from the circulating BM-derived cells, (*ii*) conventional BMT techniques can be used in clinical applications, and therefore (*iii*) fewer ethical problems arise from the treatment.

Recently Tolar et al. (35) reported that hematopoietic stem cells contributed to life prolongation in RDEB neonatal mice. Chino et al. (36) reported that treatment of embryonic BMT in RDEB mice induced the expression of donor-derived fibroblasts and type VII collagen. These reports investigated neonatal or embryonic mice and focused on type VII collagen, which is produced mainly by dermal fibroblasts. In this study we show the potential of BMT therapies in adult mice with cutaneous congenital disorders caused by deficiencies of transmembrane proteins such as COL17, which is produced mainly by keratinocytes.

As to the origin of the BM-derived cells that differentiated into epidermal cells, Tolar et al. reported that only CD150$^+$ CD48$^-$ HSCs contributed to the amelioration of RDEB mice; nevertheless, MSCs abundantly expressed type VII collagen mRNA (35). Conversely, we and other groups have reported that MSCs also have the potential to differentiate into keratinocytes (37, 38). Our experiments have shown that both HSCs and MSCs have the potential to produce Col17. However, a BMT model with infusion of enriched MSCs tended to induce more severe clinical manifestations. One hypothesis is that the infused MSCs in BMT reside so shortly that long-term effects, such as clinical improvement, might not occur (39, 40). We demonstrated that human cord blood CD34$^+$ HSCs are able to differentiate into keratinocytes in vivo. Although further investigation is needed, we suggest that the difference between the benefits of MSC and HSC transplantations owes to the lack of a long-term, renewable circulating source of Col17-producing cells induced by donor hematopoiesis. From these findings we conclude that both HSCs and MSCs contributed to the production of Col17, although HSCs played more a significant role in clinical improvement in our EB model mice.

Recently Kopp et al. (41) performed BMT and subsequent skin transplantation in one Herlitz-junctional EB infant but unfortunately the child died. They performed normal conditioning treatments similar to those used in hematological malignancies, but the treatments might be too strong for EB patients. Indeed, in our EB model mice, we had to reduce the irradiation dose before BMT to avoid erosions. This report is highly suggestive toward determining conditioning regimens.

In conclusion, we confirmed the reexpression of the previously deficient anchoring protein Col17, better clinical appearance, and longer life expectancy after BMT in our junctional EB model mice. Furthermore we demonstrated that human HSCs can contribute to the regeneration of wounded skin, producing structural proteins in the BMZ. Current conventional hematopoietic stem cell transplantation will lead to treatments for severe forms of EB or even other congenital skin disorders involving epidermal structural proteins.

Materials and Methods

Bone Marrow Transplantation. Recipient adult mice were irradiated with a lethal dose of X-rays at 9 Gy (C57BL/6 and *COL17*$^{m-/-,h+}$ mice) or 6 Gy (in *COL17*$^{m-/-}$ mice), 12 h before infusions. The 9-Gy irradiation resulted in severe erosions and hair loss within 4 wk after BMT to *COL17*$^{m-/-}$ mice. Approximately 3.0–6.0 × 10^6 murine BM-derived cells in 400 μL PBS were injected through the mouse tail vein.

Human Cord Blood Stem Cell Transplantation. Recipient adult NOG mice were irradiated with a sublethal dose of X-rays at 2.5 Gy. Twelve hours later, approximately 1.0–2.5 × 10^5 human CD34$^+$ cells in 400 μL PBS were injected through the mouse tail vein. Hematopoietic reconstitution was evaluated in peripheral blood mononuclear cells 12 wk after transplantation.

Hematopoietic and Mesenchymal Cell Transplantations. Recipient adult *COL17*$^{m-/-}$ mice were irradiated with a lethal dose of X-rays at 6 Gy. Twelve hours later, approximately 5.0 × 10^3 GFP$^+$ HSCs (n = 5) or 5.0 × 10^5 GFP$^+$ MSCs (n = 4) were mixed with 5.0 × 10^5 whole *COL17*$^{m-/-}$ BM-derived cells in 400 μL PBS and injected through the mouse tail vein.

RT-PCR Analyses. For RT-PCR, total RNA from tissues and cells was extracted using Isogen (Nippon Gene) and 200 ng of total RNA was used for cDNA synthesis in SuperScript II reverse transcriptase according to the manufacturer's instructions (Invitrogen). RT-PCR analysis of mRNA was performed in a thermocycler (GeneAmp PCR system 9600; Perkin-Elmer). The primers specific for protein sequences are summarized in Table S1. The PCR protocol for these genes included 35 cycles of amplification (denaturing at 94 °C for 1 min, annealing for 1 min, elongation at 72 °C for 1 min). Aliquots from each amplification reaction were analyzed by electrophoresis in 2% acrylamide-Tris-borate gels. Gel images were acquired and processed by an image analyzer (LAS-4000UVmini; Fujifilm).

Western Blotting. Protein lysates from epidermal tissues were subjected to SDS/PAGE and electrophoretically transferred onto a nitrocellulose membrane. The membranes were blocked with 1% nonfat dry milk in PBS, probed with rat monoclonal antibodies against mCol17 (KT4.2, 1:80,000), and then allowed to react with goat anti-rat IgG antibody coupled with HRP (1:1,000; Southern Biotech). For loading control, we used mouse anti-β-actin antibody

(1:1,000; Sigma-Aldrich) and HRP-conjugated goat anti-mouse IgG (1:1,000; Southern Biotech). The resultant immune complexes were visualized using a chemiluminescent detection system (LumiGLO; Cell Signaling Technology) and processed by an image analyzer (LAS-4000UVmini).

Ultrastructural Observations. Skin biopsy samples of two mice each from GFP$^+$ Tg mice, untreated *COL17*$^{m-/-}$ mice, and BMT-treated *COL17*$^{m-/-}$ mice were fixed in 5% glutaraldehyde solution, postfixed in 1% osmium tetroxide, dehydrated, and embedded in Epon 812. The samples were sectioned at 1-μm thickness for light microscopy and thin-sectioned at 70-nm thickness for electron microscopy. The thin sections were stained with uranyl acetate and lead citrate and examined under a transmission electron microscope (H-7100; Hitachi High-Technologies).

Clinical Evaluation of *COL17*$^{m-/-}$ Mice. After bone marrow transplantation, the clinical severity of the BMT-treated *COL17*$^{m-/-}$ mice, such as spontaneous erosions and blistering, was evaluated and compared with that of the untreated *COL17*$^{m-/-}$ mice and BMT-control mice whose donors were *COL17*$^{m-/-}$ mice. The perioral area and circumanal area tend to be naturally predisposed to erosion. We investigated the clinical severity by measuring the share of each affected area as a percent of its entire region. These were assessed by two independent assessors viewing the same clinical images. In addition we compared the vital prognosis after BMT (35 d after birth) among BMT-treated mice (n = 20), untreated *COL17*$^{m-/-}$ mice (n = 17), and BMT-control mice (n = 6).

Mechanical Rubber Stress Test. The epithelized dorsal skin areas of 1 cm^2 after erosion were marked with a pen and exposed to a mechanical rubber stress test as previously reported (18). The skin was gently stretched, and mechanical shearing forces were applied by the same investigator repeatedly (25 times) as intense, unidirectional rubbing with a pencil eraser. After 20 min, skin specimens were excised and processed for histopathological analysis. Also, we measured the total areas of erosion by ImageJ software (42).

Statistical Analyses. Mann–Whitney U test for nonparametric data, Kaplan-Meier analysis for survival curves, and log-rank test for survival evaluation were performed using Excel 2003 (Microsoft) with the add-in software Statcel2 (OMS) (43). For comparison of more than two groups, data were analyzed by Kruskal–Wallis test followed by Scheffe's F test. Results were expressed as mean ± SE.

ACKNOWLEDGMENTS. We thank Prof. K. B. Yancey (Department of Dermatology, Medical College of Wisconsin, Milwaukee, WI) for providing the *COL17*$^{m+/+,h+}$ mice, Prof. K. Owaribe (Division of Biological Science, Graduate School of Science, Nagoya University, Nagoya, Japan) for the gift of antibodies against human COL17 (D20), and Prof. T. Tanaka (Department of Dermatology, Shiga University of Medical Science, Otsu, Japan) for the gift of antibodies against mouse Col17 (KT4.2). This work was supported in part by grants-in-aid for scientific research (13357008 and 17209038 to H.S. and 15790563 to R.A.) and the Project for Realization of Regenerative Medicine (H.S.) from the Ministry of Education, Science, Sports, and Culture of Japan; by the program for Promotion of Fundamental Studies in Health Sciences of the National Institute of Biomedical Innovation (06-42 to H.S.); by Health and Labor Sciences Research Grants from the Ministry of Health, Labor, and Welfare of Japan (H13-Measures for Intractable Disease-02 and H16-Measures for Intractable Disease-02, to H.S.); and by Japanese Society of Investigative Dermatology (JSID) Fellowship Shiseido Award 2007 (to R.A.).

1. Satake K, Lou J, Lenke LG (2004) Migration of mesenchymal stem cells through cerebrospinal fluid into injured spinal cord tissue. *Spine (Phila Pa 1976)* 29:1971–1979.
2. Herzog EL, Chai L, Krause DS (2003) Plasticity of marrow-derived stem cells. *Blood* 102: 3483–3493.
3. Jiang Y, et al. (2002) Pluripotency of mesenchymal stem cells derived from adult marrow. *Nature* 418:41–49.
4. Orlic D, et al. (2001) Bone marrow cells regenerate infarcted myocardium. *Nature* 410: 701–705.
5. Kocher AA, et al. (2001) Neovascularization of ischemic myocardium by human bone-marrow-derived angioblasts prevents cardiomyocyte apoptosis, reduces remodeling and improves cardiac function. *Nat Med* 7:430–436.
6. Ferrari G, et al. (1998) Muscle regeneration by bone marrow-derived myogenic progenitors. *Science* 279:1528–1530.
7. Yamada M, et al. (2004) Bone marrow-derived progenitor cells are important for lung repair after lipopolysaccharide-induced lung injury. *J Immunol* 172:1266–1272.
8. Kale S, et al. (2003) Bone marrow stem cells contribute to repair of the ischemically injured renal tubule. *J Clin Invest* 112:42–49.
9. Wagers AJ, Sherwood RI, Christensen JL, Weissman IL (2002) Little evidence for developmental plasticity of adult hematopoietic stem cells. *Science* 297:2256–2259.
10. Lagasse E, et al. (2000) Purified hematopoietic stem cells can differentiate into hepatocytes in vivo. *Nat Med* 6:1229–1234.
11. Fine JD, et al. (2008) The classification of inherited epidermolysis bullosa (EB): Report of the Third International Consensus Meeting on Diagnosis and Classification of EB. *J Am Acad Dermatol* 58:931–950.
12. Mavilio F, et al. (2006) Correction of junctional epidermolysis bullosa by transplantation of genetically modified epidermal stem cells. *Nat Med* 12:1397–1402.
13. Banasik MB, McCray PB, Jr (2010) Integrase-defective lentiviral vectors: Progress and applications. *Gene Ther* 17:150–157.
14. Murata H, et al. (2007) Donor-derived cells and human graft-versus-host disease of the skin. *Blood* 109:2663–2665.
15. Harris RG, et al. (2004) Lack of a fusion requirement for development of bone marrow-derived epithelia. *Science* 305:90–93.
16. Inokuma D, et al. (2006) CTACK/CCL27 accelerates skin regeneration via accumulation of bone marrow-derived keratinocytes. *Stem Cells* 24:2810–2816.
17. Nishie W, et al. (2007) Humanization of autoantigen. *Nat Med* 13:378–383.
18. Fritsch A, et al. (2008) A hypomorphic mouse model of dystrophic epidermolysis bullosa reveals mechanisms of disease and response to fibroblast therapy. *J Clin Invest* 118:1669–1679.
19. Ito M, et al. (2002) NOD/SCID/gamma(c)(null) mouse: An excellent recipient mouse model for engraftment of human cells. *Blood* 100:3175–3182.
20. Bauer JW, Lanschuetzer C (2003) Type XVII collagen gene mutations in junctional epidermolysis bullosa and prospects for gene therapy. *Clin Exp Dermatol* 28:53–60.
21. Robbins PB, Sheu SM, Goodnough JB, Khavari PA (2001) Impact of laminin 5 beta3 gene versus protein replacement on gene expression patterns in junctional epidermolysis bullosa. *Hum Gene Ther* 12:1443–1448.
22. Robbins PB, et al. (2001) In vivo restoration of laminin 5 beta 3 expression and function in junctional epidermolysis bullosa. *Proc Natl Acad Sci USA* 98:5193–5198.
23. Dellambra E, et al. (2001) Gene correction of integrin beta4-dependent pyloric atresia-junctional epidermolysis bullosa keratinocytes establishes a role for beta4 tyrosines 1422 and 1440 in hemidesmosome assembly. *J Biol Chem* 276:41336–41342.
24. Seitz CS, Giudice GJ, Balding SD, Marinkovich MP, Khavari PA (1999) BP180 gene delivery in junctional epidermolysis bullosa. *Gene Ther* 6:42–47.
25. Igoucheva O, Kelly A, Uitto J, Alexeev V (2008) Protein therapeutics for junctional epidermolysis bullosa: Incorporation of recombinant beta3 chain into laminin 332 in beta3-/- keratinocytes in vitro. *J Invest Dermatol* 128:1476–1486.
26. Woodley DT, et al. (2004) Injection of recombinant human type VII collagen restores collagen function in dystrophic epidermolysis bullosa. *Nat Med* 10:693–695.
27. Wong T, et al. (2008) Potential of fibroblast cell therapy for recessive dystrophic epidermolysis bullosa. *J Invest Dermatol* 128:2179–2189.
28. Woodley DT, et al. (2007) Intravenously injected human fibroblasts home to skin wounds, deliver type VII collagen, and promote wound healing. *Mol Ther* 15:628–635.
29. Hobbs JR, et al. (1981) Reversal of clinical features of Hurler's disease and biochemical improvement after treatment by bone-marrow transplantation. *Lancet* 2:709–712.
30. Sands MS, et al. (1997) Murine mucopolysaccharidosis type VII: Long term therapeutic effects of enzyme replacement and enzyme replacement followed by bone marrow transplantation. *J Clin Invest* 99:1596–1605.
31. Warkentin PI, Dixon MS, Jr, Schafer I, Strandjord SE, Coccia PF (1986) Bone marrow transplantation in Hunter syndrome: A preliminary report. *Birth Defects Orig Artic Ser* 22:31–39.
32. Krivit W, et al. (1984) Bone-marrow transplantation in the Maroteaux-Lamy syndrome (mucopolysaccharidosis type VI). Biochemical and clinical status 24 months after transplantation. *N Engl J Med* 311:1606–1611.
33. Gasper PW, et al. (1984) Correction of feline arylsulphatase B deficiency (mucopolysaccharidosis VI) by bone marrow transplantation. *Nature* 312:467–469.
34. Sampaolesi M, et al. (2006) Mesoangioblast stem cells ameliorate muscle function in dystrophic dogs. *Nature* 444:574–579.
35. Tolar J, et al. (2009) Amelioration of epidermolysis bullosa by transfer of wild-type bone marrow cells. *Blood* 113:1167–1174.
36. Chino T, et al. (2008) Bone marrow cell transfer into fetal circulation can ameliorate genetic skin diseases by providing fibroblasts to the skin and inducing immune tolerance. *Am J Pathol* 173:803–814.
37. Wu Y, Chen L, Scott PG, Tredget EE (2007) Mesenchymal stem cells enhance wound healing through differentiation and angiogenesis. *Stem Cells* 25:2648–2659.
38. Sasaki M, et al. (2008) Mesenchymal stem cells are recruited into wounded skin and contribute to wound repair by transdifferentiation into multiple skin cell type. *J Immunol* 180:2581–2587.
39. Rieger K, et al. (2005) Mesenchymal stem cells remain of host origin even a long time after allogeneic peripheral blood stem cell or bone marrow transplantation. *Exp Hematol* 33:605–611.
40. Dickhut A, et al. (2005) Mesenchymal stem cells obtained after bone marrow transplantation or peripheral blood stem cell transplantation originate from host tissue. *Ann Hematol* 84:722–727.
41. Kopp J, et al. (2005) Hematopoietic stem cell transplantation and subsequent 80% skin exchange by grafts from the same donor in a patient with Herlitz disease. *Transplantation* 79:255–256.
42. Abramoff MD, Magelhaes PJ, Ram SJ (2004) Image Processing with ImageJ. *Biophotonics International* 11:36–42.
43. Yanai H (2004) *Statcel-The Useful Add-In Software Forms on Excel* (OMS, Tokyo) 2nd Ed.

Corrections and Retraction

CORRECTIONS

GENETICS

Correction for "Lack of association of common variants on chromosome 2p with primary open-angle glaucoma in the Japanese population," by Fumihiko Mabuchi, Yoichi Sakurada, Kenji Kashiwagi, Zentaro Yamagata, Hiroyuki lijima, and Shigeo Tsukahara, which appeared in issue 21, May 25, 2010, of *Proc Natl Acad Sci USA* (107:E90–E91; first published April 27, 2010; 10.1073/pnas.0914903107).

The authors note that, due to a printer's error, the author name Hiroyuki lijima should have appeared as Hiroyuki Iijima. The corrected author line appears below. The online version has been corrected.

Fumihiko Mabuchi[a,1], Yoichi Sakurada[a], Kenji Kashiwagi[a], Zentaro Yamagata[b], Hiroyuki Iijima[a], and Shigeo Tsukahara[a]

www.pnas.org/cgi/doi/10.1073/pnas.1008743107

MEDICAL SCIENCES

Correction for "Bone marrow transplantation restores epidermal basement membrane protein expression and rescues epidermolysis bullosa model mice," by Yasuyuki Fujita, Riichiro Abe, Daisuke Inokuma, Mikako Sasaki, Daichi Hoshina, Ken Natsuga, Wataru Nishie, James R. McMillan, Hideki Nakamura, Tadamichi Shimizu, Masashi Akiyama, Daisuke Sawamura, and Hiroshi Shimizu, which appeared in issue 32, August 10, 2010, of *Proc Natl Acad Sci USA* (107:14345–14350; first published July 26, 2010; 10.1073/pnas.1000044107).

The authors note that, due to a printer's error, Yasuyuki Fujita was omitted as the first author of this article. The corrected author line appears below. The online and print versions have been corrected.

Yasuyuki Fujita[a], Riichiro Abe[a,1], Daisuke Inokuma[a], Mikako Sasaki[a], Daichi Hoshina[a], Ken Natsuga[a], Wataru Nishie[a], James R. McMillan[a], Hideki Nakamura[a], Tadamichi Shimizu[b], Masashi Akiyama[a], Daisuke Sawamura[c], and Hiroshi Shimizu[a,1]

www.pnas.org/cgi/doi/10.1073/pnas.1011158107

RETRACTION

MEDICAL SCIENCES

Retraction for "Complete and persistent phenotypic correction of phenylketonuria in mice by site-specific genome integration of murine phenylalanine hydroxylase cDNA," by Li Chen and Savio L. C. Woo, which appeared in issue 43, October 25, 2005, of *Proc Natl Acad Sci USA* (102:15581–15586; first published October 17, 2005; 10.1073/pnas.0503877102).

The undersigned author wishes to note the following: "After re-examining the laboratory records, I have concluded that there are data irregularities underlying this paper that warrant its retraction. I regret not recognizing these irregularities before the manuscript was published and apologize for any inconvenience this might have caused."

Savio L. C. Woo

www.pnas.org/cgi/doi/10.1073/pnas.1009071107

Journal of Dermatological Science 57 (2010) 183–191

Contents lists available at ScienceDirect

Journal of Dermatological Science

journal homepage: www.elsevier.com/jds

Topical application of anti-angiogenic peptides based on pigment epithelium-derived factor can improve psoriasis

Riichiro Abe [a,1,*], Sho-ichi Yamagishi [b,1], Yasuyuki Fujita [a], Daichi Hoshina [a], Mikako Sasaki [a], Kazuo Nakamura [b], Takanori Matsui [b], Tadamichi Shimizu [c], Richard Bucala [d], Hiroshi Shimizu [a]

[a] Department of Dermatology, Hokkaido University Graduate School of Medicine, Sapporo, Japan
[b] Department of Pathophysiology and Therapeutics of Diabetic Vascular Complications, Kurume University School of Medicine, Kurume, Japan
[c] Department of Dermatology, Toyama University School of Medicine, Toyama, Japan
[d] Department of Internal Medicine, Yale University School of Medicine, New Haven, CT, USA

ARTICLE INFO

Article history:
Received 5 August 2009
Received in revised form 17 December 2009
Accepted 17 December 2009

Keywords:
Angiogenesis
Keratinocyte
Psoriasis
Pigment epithelium-derived factor
Vascular endothelial growth factor

ABSTRACT

Background: Psoriasis is a common chronic inflammatory skin disorder with a high prevalence (3–5%) in the Caucasian population. Although the number of capillary vessels increases in psoriatic lesions, there have been few reports that have specifically examined the role of angiogenesis in psoriasis. Angiogenic factors, such as vascular endothelial growth factor (VEGF), may dominate the activity of anti-angiogenic factors and accelerate angiogenesis in psoriatic skin.
Objective: We investigated to identify small peptide mimetics of PEDF that might show anti-angiogenic potential for the topical treatment for psoriasis.
Methods: We examined the expression of PEDF in skin by immunohistochemical staining, immunoblotting, and RT-PCR. To identify potential PEDF peptides, we screened peptides derived from the proteolytic fragmentation of PEDF for their anti-proliferative action. Anti-psoriatic functions of these peptides were analyzed using a mouse graft model of psoriasis.
Results: The specific low-molecular weight peptides (MW < 850 Da) penetrated the skin and showed significant anti-angiogenic activity in vitro. Topical application of these peptides in a severe combined immunodeficient mouse model of psoriatic disease led to reduced angiogenesis and epidermal thickness.
Conclusions: These data suggest that low-molecular PEDF peptides with anti-angiogenic activity may be a novel therapeutic strategy for psoriasis.

1. Introduction

Psoriasis is a common skin disease affecting 0.5–3% of the Caucasian population [1]. Histopathologically, this disorder is characterized by accelerated epidermal proliferation, by the infiltration of inflammatory cells into the epidermis and upper dermis, and by telangiectasia in the superficial dermis. Although the molecular pathogenesis of psoriasis remains unclear, several hypotheses have been proposed. Activated T lymphocytes infiltrate into the lesional skin areas where they secrete a variety of cytokines such as tumor necrosis factor (TNF)-α, interferon-γ, IL-2 and IL-12, and thus play an important role in psoriatic inflammatory changes [2]. In addition, epidermal proliferation is influenced by inappropriate vascular expansion in the superficial dermis [3]. Furthermore, these microvascular changes in psoriatic skin lesions include pronounced capillary dilatation, increased vessel permeability and endothelial cell proliferation and protrusion into the dermal papillae capillaries. Therefore inappropriate angiogenic growth has been proposed to contribute to the pathogenesis of psoriasis [4,5]. The overexpression of angiogenic factors also occurs; for instance, vascular endothelial growth factor (VEGF) is strongly up-regulated in psoriatic skin lesions [6].

There have been a number of therapeutic strategies devised for psoriasis. Topical steroids, topical vitamin D3 analogs, oral retinoids, UV irradiation such as PUVA and narrow-band UVB, cyclosporine and other immunosuppressants have been widely used. In addition, biological agents that target cytokines such as TNF-α have recently been developed [7]. Most strategies are aimed at reducing the inflammatory reaction and epidermal proliferation, but yet there have been few agents targeting angiogenesis in psoriasis.

Pigment epithelium-derived factor (PEDF) is a glycoprotein that belongs to the superfamily of serine protease inhibitors, and it was

Abbreviations: PEDF, pigmented epithelium-derived factor; VEGF, vascular endothelial growth factor.

* Corresponding author at: Department of Dermatology, Hokkaido University Graduate School of Medicine, N 15 W 7, Kita-ku, Sapporo 060-8638, Japan. Tel.: +81 11 706 7387; fax: +81 11 706 7820.
E-mail address: aberi@med.hokudai.ac.jp (R. Abe).
[1] These authors contributed equally to this paper.

0923-1811/$36.00
doi:10.1016/j.jdermsci.2009.12.010

first identified as a retinal pigment epithelium-derived protein with neuronal differentiating activity [8]. Recently, PEDF has been shown to have potent anti-angiogenic activity in cell culture and in animal models. PEDF inhibits retinal endothelial cell growth and migration, and it suppresses ischemia-induced retinal neovascularization [9]. In addition, we reported that PEDF inhibits malignant melanoma growth by suppressing tumor angiogenesis [10]. These observations led us to hypothesize that an imbalance in anti-angiogenic factors potentially involving PEDF may contribute to the pathogenesis of psoriasis. PEDF also shows anti-inflammatory activity, suggesting an additional, ameliorative role in the control of inflammation and keratinocyte proliferation.

In this study, we examined PEDF protein production in psoriasis lesions and in normal skin, and we investigated the effect of PEDF on keratinocyte proliferation in vitro and on psoriatic skin in a murine xenograft model. We also report the identification of low molecular weight PEDF peptides that show anti-angiogenic activity after topical application.

2. Experimental procedures

2.1. Patients

Sera were obtained from 21 psoriasis patients (13 males and 8 females, and mean age 46.9 years) and 14 healthy volunteers (males 7 and females 7, and mean age 42.2 years) from the Department of Dermatology, Hokkaido University Hospital. The diagnosis of psoriasis was made on the basis of clinical images and histopathological findings from skin biopsies. The enrolled patients had generalized plaque psoriasis, which were evaluated by a single qualified dermatologist. Three skin tissue specimens were obtained from each psoriatic lesion. Normal skin tissues also were obtained from healthy volunteers. Informed consent was obtained from each volunteer according to the Declaration of Helsinki Principles. All the experiments using human samples were performed under the approval of the ethical committee of Hokkaido University.

2.2. Experimental mice

The C.B-17/Icr-scid/scidJcl SCID mouse (Clea, Tokyo, Japan) was used for xenotransplantation experiments. All the animal experiments were performed under the approval of the ethical committee for animal studies in Hokkaido University.

2.3. Immunohistochemistry

The paraffin-embedded skin tissues from psoriasis patients were cut into 4 μm-thick sections. The sections were deparaffinized, incubated with 0.1% trypsin at 37 °C for 15 min. Endogenous peroxidase activity was inhibited by pretreatment with 3% hydrogen peroxide. The sections were then treated with 10% normal goat serum at room temperature for 30 min, followed by incubation with the anti-PEDF antibody (Santa Cruz Biotechnology, Santa Cruz, CA) at 4 °C overnight. After washing, the sections were incubated with horseradish peroxidase (HRP)-conjugated goat anti-rabbit IgG at room temperature for 30 min and the PEDF-positive staining visualized with diaminobenzidine (Dojin, Kumamoto, Japan) as a chromogen and hematoxylin as a counterstain.

For immunofluorescence, skin tissues were immediately embedded in optimal cutting temperature (OCT) reagent (Sakura Finetechnical, Tokyo, Japan) and snap-frozen in liquid nitrogen. Cryosections of 5 μm were prepared, washed with PBS, and then fixed in cold acetone for 10 min at −20 °C. Primary and secondary antibodies were applied at room temperature for 1 h. The sections were finally washed with PBS and mounted on microscope slides. The samples were analyzed using a Fluoview confocal laser scanning microscope (Olympus, Nagano, Japan). The following antibodies were used: rat anti-mouse CD31 antibody, anti-mouse CD3 antibody, anti-mouse Gr-1 antibody, and anti-mouse CD11b antibody (BD Biosciences, San Jose, CA), rabbit polyclonal anti-pankeratin antibody (PROGEN Biotechnik, Heidelberg, Germany), rabbit polyclonal anti-Ki67 antibody (Novocastra, Newcastle, UK), FITC-conjugated goat anti-rabbit antibody, FITC-conjugated goat anti-rat antibody (Jackson ImmunoResearch, West Grove, PA), TRITC-conjugated anti-rabbit antibody (Southern Biotechnology Associates, Birmingham, AL).

2.4. Immunoblots

Skin tissues of normal volunteers and psoriasis patients were treated with 1 M sodium hydroxide at 4 °C overnight, and the epidermal sheets easily removed from the dermal components. These tissues were frozen and then homogenized in PBS. Samples obtained from epidermis and dermis were electrophoresed on SDS–PAGE. Proteins on the gel were electrophoretically transferred to a nitrocellulose membrane (Bio-Rad, Hercules, CA) and the membranes probed with first antibody at 4 °C overnight, washed three times for 5 min, and then incubated with HRP-conjugated secondary antibodies at room temperature for 1 h. Proteins were visualized with a Konica immunostaining kit (Konica, Tokyo, Japan). The following antibodies were used: anti-PEDF and anti-VEGF rabbit polyclonal antibody (Santa Cruz Biotechnology), anti-α-tubulin mouse monoclonal antibody (Sigma, St. Louis, MO), HRP-conjugated goat anti-rabbit IgG, and HRP-conjugated goat anti-mouse IgG (Biosource, Camarillo, CA). We used anti-PEDF at 1:200, and the secondary antibodies at 1:1000 dilutions.

2.5. RT-PCR analysis

RNA (0.5 μg) was used to produce cDNA using a reverse transcription kit (Sigma, Poole, Dorset, United Kingdom). PCR was done using a 2400 thermocycler (Perkin-Elmer, Norwalk CT) with conditions set to 40 s at 94 °C, 60 s at 55 °C, and 60 s at 72 °C (30 cycles). The quality of DNA was verified by 0.59 kb β-actin PCR products using primers (forward 5′-ATGATATCGCCGCGCTCGTC-3′; reverse 5′-CGCTCGGTGAGGATCTTCA-3′). PEDF forward and reverse primers were 5′-GGTGCTACTCCTCTGCATT-3′ and 5′-ACTGAACCTGACCGTACAAGAAAGGATCCTCCTCCTC-3′. PCR products were separated by 2% agarose gel and visualized under UV light following ethidium bromide staining.

2.6. Preparations of PEDF proteins

The PEDF proteins were purified as described previously [9]. Briefly, 293T cells (ATCC, Rockville, MD, USA) were transfected with the recombinant vector pBK-CMV-C terminally hexahistidine-tagged PEDF using FuGENE® 6 transfection reagent (Roche Diagnostics, Mannheim, Germany) according to the manufacturer's instructions. The PEDF proteins were purified from conditioned media by a Ni-NTA spin kit (Qiagen, Hilden, Germany) according to the manufacturer's recommendation. Sodium dodecyl sulphate–polyacrylamide gel electrophoresis (SDS–PAGE) of purified PEDF proteins revealed a single band with a molecular mass of about 50 kDa, which showed positive reactivity with monoclonal antibodies directed against human PEDF (Transgenic, Kumamoto, Japan).

2.7. PEDF enzyme-linked immunosorbent assay

A PEDF enzyme-linked immunosorbent assay was performed as previously reported [11]. Briefly, a 96-well microtiter plate (Nalge

Nunc International, Rochester, NY) was coated by overnight incubation with anti-PEDF monoclonal antibody (Transgenic, Kumamoto, Japan). Samples were diluted 50-fold in 10 mM PBS pH 7.4, 0.25% BSA and 0.05% Tween-20, and then incubated at room temperature for 2 h. After washing, a biotinylated anti-human PEDF polyclonal antibody (R&D Systems, Minneapolis, MN) was added and incubation continued for 2 h at room temperature. The plate was then incubated with HRP-conjugated streptavidine solution (Zymed, South San Francisco, CA) at room temperature for 30 min. After washing, the chromogenic substrate solution (Dako, Tokyo, Japan) was added and the plate was incubated at room temperature for 15 min. Optical densities were measured at 450 nm and protein concentrations calculated from a standard curve generated by a curve-fitting program (Berthold Technology, Bad Wildbad, Germany).

2.8. PEDF secretion from cultured keratinocytes and fibroblasts

Normal human epidermal keratinocytes (NHEKs) were purchased from Clontech (Mountain View, CA and cultured in KGM® medium (Cambrex, East Rutherford, NJ) until 70% confluence. Normal human fibroblasts were purchased from Dainippon Seiyaku (Osaka, Japan) and cultured in Dulbecco's Modified Eagle's Medium (DMEM) (Invitrogen, Carlsbad, CA) containing 10% FBS, 1% penicillin, 1% streptomycin and 1% amphotericin B until 70% confluence. The cells were expanded in 12 cm sterile culture dish with 10 ml of medium, and then stimulated with lipopolysaccharide (Sigma) at 37 °C for 72 h. Media was collected 1 day after stimulation. PEDF concentrations in collected medium were assessed by ELISA as described above.

2.9. Keratinocyte proliferation assay

NHEKs were seeded into 96-well plates at a concentration of 10^3 cells in 100 μl of medium per well. After cultivation with 1, 10, 100 nM recombinant PEDF [12] and/or 100 ng/ml recombinant VEGF (R&D systems) for 2 and 4 days, 10 μl of Cell Counting Kit (Dojin) was added to each well. After incubation for 2 h, the absorbance at 450 nm was measured on a microplate reader.

2.10. Treatment of the grafted skin lesions with recombinant PEDF

A graft bed of approximately 1 cm^2 was created on the shaved area of the back of a 7 to 8-week-old anesthetized SCID mouse by removing the full-thickness skin and keeping the vessel plexus intact on the fascia overlying back muscles. The human skin obtained by biopsy was washed in PBS containing 1% penicillin, 1% streptomycin and 1% amphotericin B, and fatty deposits were removed by gentle dissection. The full-thickness human skin graft was placed onto wound bed. The transplants were held in place using 5/0 silk suture material, and 1% gentamicin sulfate ointment was applied. The graft was covered with an adhesive wound

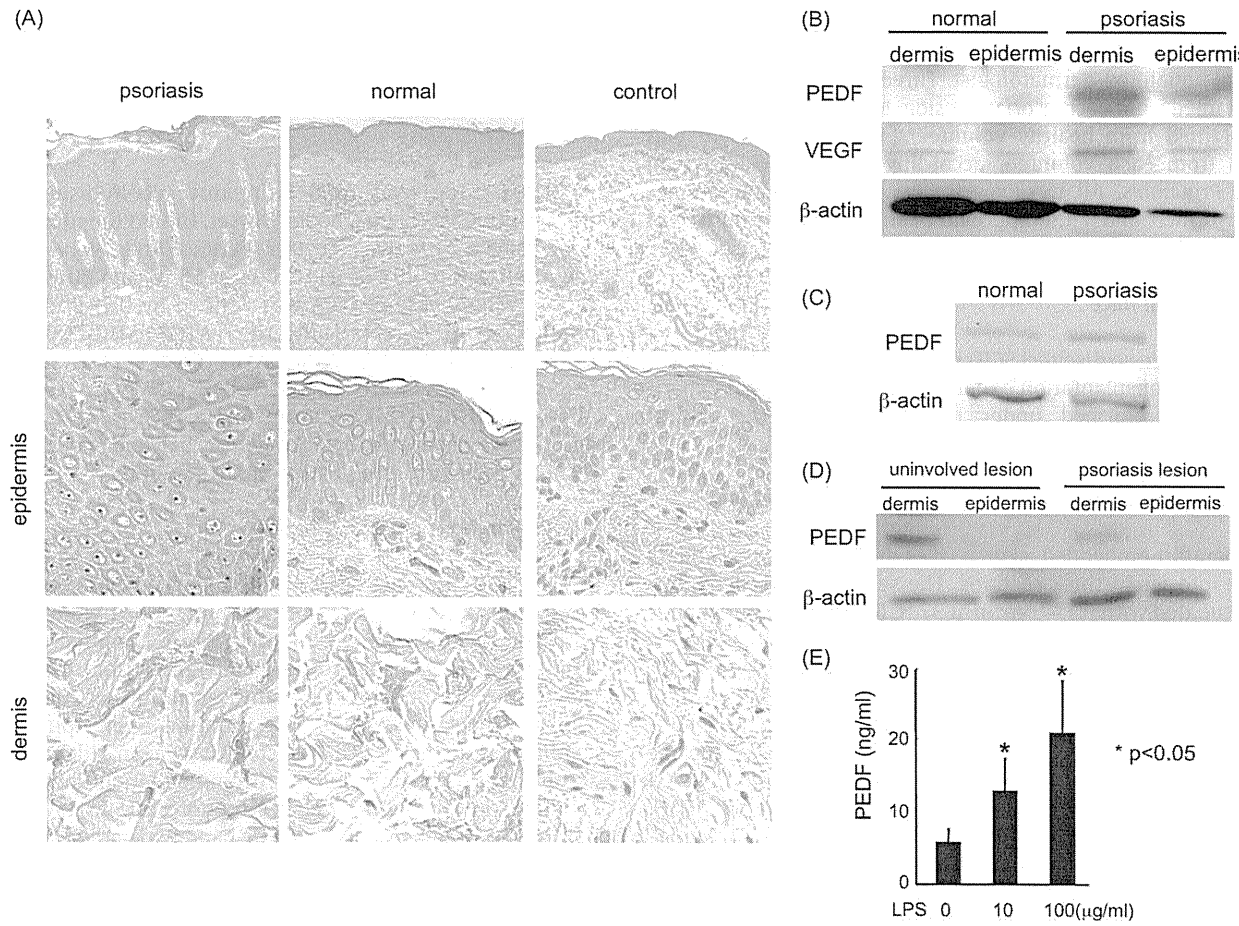

Fig. 1. PEDF is expressed in both the epidermis and dermis. (A) Immunohistochemistry of normal and psoriatic skin lesions. In normal skin, PEDF was detected in both the epidermis and the dermis. PEDF was significantly up-regulated in psoriatic epidermis in comparison with normal epidermis. (B) The expression of PEDF protein was up-regulated in psoriasis lesions. Positive bands were identified with a molecular weight of about 50 kDa from both the epidermis and dermis, which corresponds to the molecular weight of PEDF. (C) PEDF mRNA levels were analyzed using RT-PCR. The expression of PEDF mRNA was slightly up-regulated in psoriasis lesions compared to that of normal skin. (D) The expression of PEDF protein was up-regulated in uninvolved lesion of psoriasis patient compared to psoriasis lesion. (E) The levels of PEDF in the supernatants of cultured normal human keratinocytes were assessed by ELISA. LPS (10 or 100 μg/ml) was used to stimulate keratinocyte production of PEDF ($^*p < 0.05$).

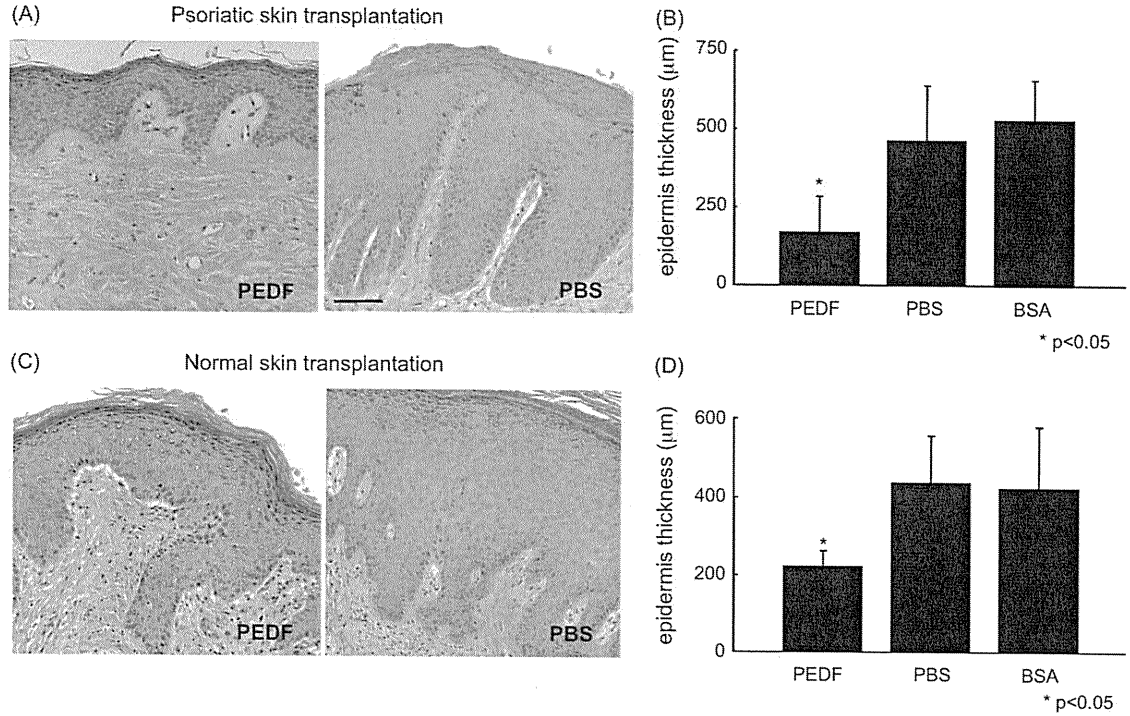

Fig. 2. Intradermal PEDF administration reduced the thickness of grafted epidermis in xenotransplanted SCID mice. Acanthosis was significantly reduced both in psoriatic (A, B) and normal (C, D) skin when compared to PBS or BSA injected groups. Scale bar, 50 μm. Values shown are means and SDs based on four to six measurements per histological section in four histological sections per mouse from duplicate mice transplanted with skin samples from four donors ($^*p < 0.05$).

dressing and then with a standard bandage. Dressing material and sutures were removed 7 days after transplantation.

Grafted mice received recombinant PEDF in 50 μl of PBS by intradermal injection around the xenograft lesion at 30 μg/mouse every three days for three weeks. The PEDF dose was well tolerated without any evident side effects. Mice in the control group received the same volume of PBS or BSA (30 μg). The day after the last injection, biopsies were collected from the transplants from both treatment and control groups. The skin tissues were immediately embedded in OCT reagent and snap-frozen in liquid nitrogen. Cryosections of 5 μm were then prepared for histological and immunohistochemical staining.

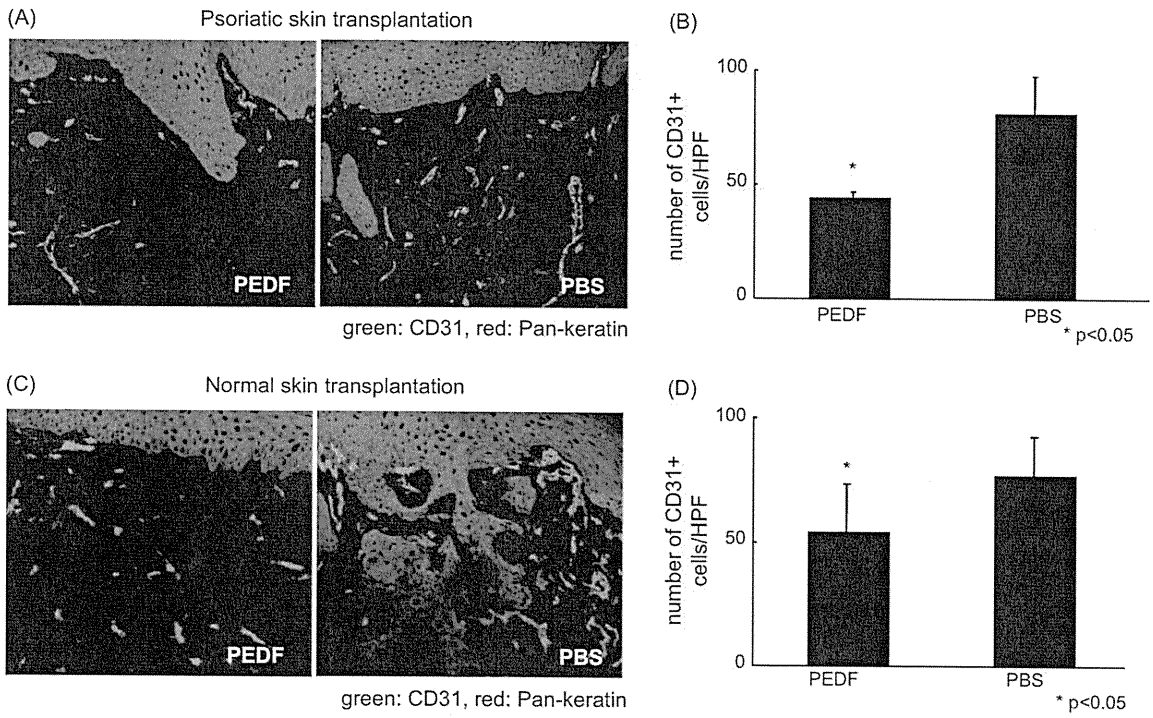

Fig. 3. Intradermal PEDF administration reduced angiogenesis of grafted epidermis. CD31-positive cells (capillary endothelial cells) were enumerated by immunofluorescence after the treatment of psoriatic (A, B) and normal skin (C, D) with PEDF or PBS. Quantification of CD31-positive blood vessels per 100× microscopic field in human skin grafted areas. The data are presented as mean CD31-positive blood vessel numbers per 100× microscopic field, ±SD ($^*p < 0.05$).

2.11. Identification of functional PEDF peptides

Full-length human PEDF cDNA was divided into three parts. Polymerase chain reaction (PCR) products digested by NdeI and SalI were ligated into the multiple cloning site of expression vector pGEX-6P-1 (Amersham Biosciences, Buckinghamshire, United Kingdom). Sequences of the sense and antisense primers were: 5′-AAACATATGCAGGCCCTGGTGCTACTCCTCTGCAT-3′ and 5′-CCCGTCGACTTATGACTTTTCCAGAGGTGCCACAAA-3′ for amplifying F1 cDNA fragment, 5′-AAACATATGTATGGGACCAGGCCCAGAGTCCTGA-3′ and 5′-CCCGTCGACTTAGTCATGAATGAACTCGGAGGTGA-3′ for F2, and 5′-GGGCATATGATAGACCGAGAACTGAAGACCGTGCA-3′ and 5′-AAAGTCGACTTAGGGGCCCCTGGGGTCCAGAAT-3′ for F3. Each human PEDF fragment was purified according to the method of Walker et al. [13]. Human PEDF peptides (see Fig. 6) were synthesized (Sigma–Aldrich, Tokyo, Japan). MG63 human osteosarcoma cells (Health Science Research Resources Bank, Tokyo, Japan) were maintained in Dulbecco's modified Eagle's medium (DMEM) supplemented with 10% of fetal bovine serum (FBS) (ICN Biomedicals Inc., Aurora, OH, USA) and 100 units/ml penicillin/streptomycin. PEDF fragment or peptide treatment was carried out in a medium containing 0.1% of FBS. HUVECs and MG63 cells were treated with or without 100 nM PEDF protein, fragments (F1–F3) or peptides (P1–P6, P5–1, P5–2, and P5–3) or VEGF (25 ng/ml) for 24 h. HUVECs additionally were treated with 100 ng/ml recombinant VEGF (R&D systems) for 2 and 4 days. Cells were incubated with [^{3}H]thymidine (Amersham Bioscience) or 5-bromo-2′deoxyuridine (BrdU) (Roche, Basel, Switzerland) for the last 4 h of culture and proliferation assessed as described previously [14,15].

For the analysis of p21 production, 50 μg of whole cell lysates were prepared and assayed for the expression of p21 and β-actin by Western blotting. Reaction with antibodies and detection with an enhanced chemiluminescence detection system (Amersham Biosciences) were performed as described previously [16].

2.12. Skin penetration of topical applied PEDF peptide

Biotin-labeled PEDF peptide (Sigma–Aldrich) was dissolved in PBS (1 mM) and 70 μl applied to the mouse skin. After 2 h, the applied site was removed and localization in the skin was determined by rhodamine–avidin staining (BD Biosciences). CD31 staining (BD Biosciences) was performed simultaneously and the samples analyzed using a Fluoview confocal laser scanning microscope (Olympus). The experiments of peptide application were repeated 3 times, and 3 mice were used in each experiment.

2.13. Treatment of the grafted psoriatic lesions with PEDF peptide

PEDF peptide was dissolved in PBS (1 mM) and 70 μl of the solution was applied on the grafted site daily for 14 days. No side effects were apparent at the applied sites. Mice in the control group received the same volume of PBS. Biopsies were collected on the day following the last injections and analyzed as described above.

2.14. Statistical analysis

Data were analyzed using unpaired, 2-tailed Student's *t* test. A *p* value less than 0.05 was considered significant.

3. Results

3.1. PEDF is highly expressed in epidermal psoriasis lesions

Immunohistochemical analysis revealed that PEDF protein is present in the cytoplasm of keratinocytes of both psoriatic and normal skin (Fig. 1A). In the dermis, fibroblasts also were positive for PEDF, but the staining was less intense than in the epidermis. Western blotting analysis of human epidermal and dermal proteins revealed a single band with a molecular weight of about 50 kDa (Fig. 1B). PEDF protein and mRNA levels were significantly higher in psoriasis lesions when compared to normal skin (Fig. 1C).

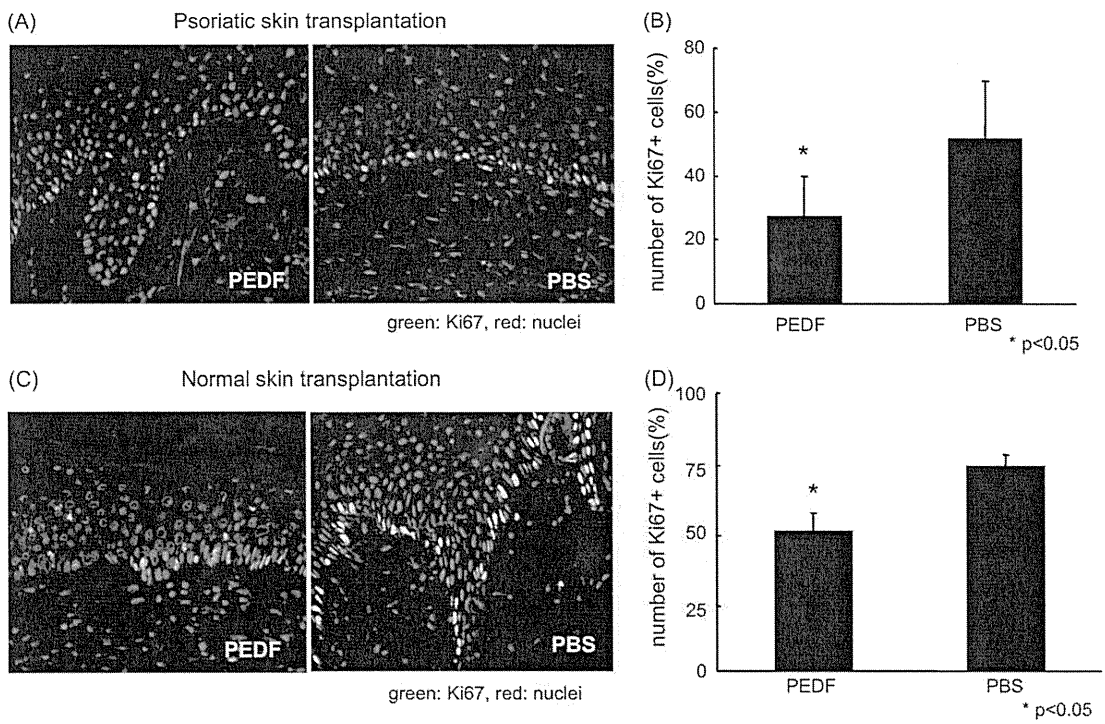

Fig. 4. Epidermal proliferation in basal keratinocytes is inhibited by PEDF. Ki-67-positive (proliferating) cells were stained and enumerated by immunofluorescence after the treatment of psoriatic (A, B) and normal skin (C, D) with PEDF or PBS. The Ki-67-positive keratinocytes in the basal layer were enumerated and the percentage of Ki-67-positive cells in basal layer calculated (*$p < 0.05$).

Interestingly, PEDF protein levels of uninvolved lesion of psoriasis patient were higher than that in psoriasis lesions (Fig. 1D). VEGF also was increased in psoriatic skin, which is consistent with prior reports [6].

3.2. PEDF secretion from cultured keratinocytes after lipopolysaccharide stimulation

PEDF was constitutively secreted by cultured keratinocytes (Fig. 1E) and after LPS stimulation, its secretion was significantly up-regulated in a dose-dependent manner ($p < 0.05$). Fibroblasts by contrast failed to show up-regulation of PEDF secretion after LPS or IL-1β stimulation (data not shown). These results imply that keratinocytes but not fibroblasts secrete PEDF in a regulated fashion in response to inflammatory stimulation. These data contrast with a prior report that PEDF is detected primarily in the dermis, with little protein evident in the epidermal layers [17].

3.3. PEDF levels in serum of psoriasis patients and normal controls

Serum VEGF levels have previously been reported to be significantly elevated in psoriasis patients [6]. If elevated serum VEGF values reflect cytokine overproduction in the skin that then enters the systemic circulation, the pathogenesis in psoriasis might relate not only to a disruption of local angiogenesis in the skin but also to angiogenesis at the systemic level. We next examined whether serum PEDF serum levels also were elevated in psoriasis patients, however we observed no significant difference in PEDF levels between psoriasis patients (14.9 ± 4.1 μg/ml) ($n = 21$) and normal controls (15.1 ± 2.9 μg/ml) ($n = 14$). Furthermore there is no correlation between psoriasis severity and serum PEDF concentration.

3.4. Intradermal injection of PEDF reduces acanthosis, dermal angiogenesis and keratinocyte proliferation of grafted skin by

We hypothesized that PEDF produced by keratinocytes not only regulates local angiogenesis, but also suppresses epidermal proliferation and the resulting acanthosis in psoriatic inflammatory lesions. To investigate this possibility *in vivo*, we studied a psoriasis graft model in which patient-derived skin is xenografted onto severe combined immunodeficient (SCID) mice. Recombinant PEDF (30 μg) was injected intradermally in the area of the graft for three weeks and epidermal thickness evaluated histopathologically. The epidermal thickness of the grafted area was significantly reduced after treatment with PEDF when compared to BSA or PBS treated controls (Fig. 2). Injections of equivalent amounts of BSA, as a non-specific protein control, did not reduce epidermal thickness. Normal human skin transplanted to SCID mice also showed a reduction of epidermal thickness after PEDF-treatment. On the

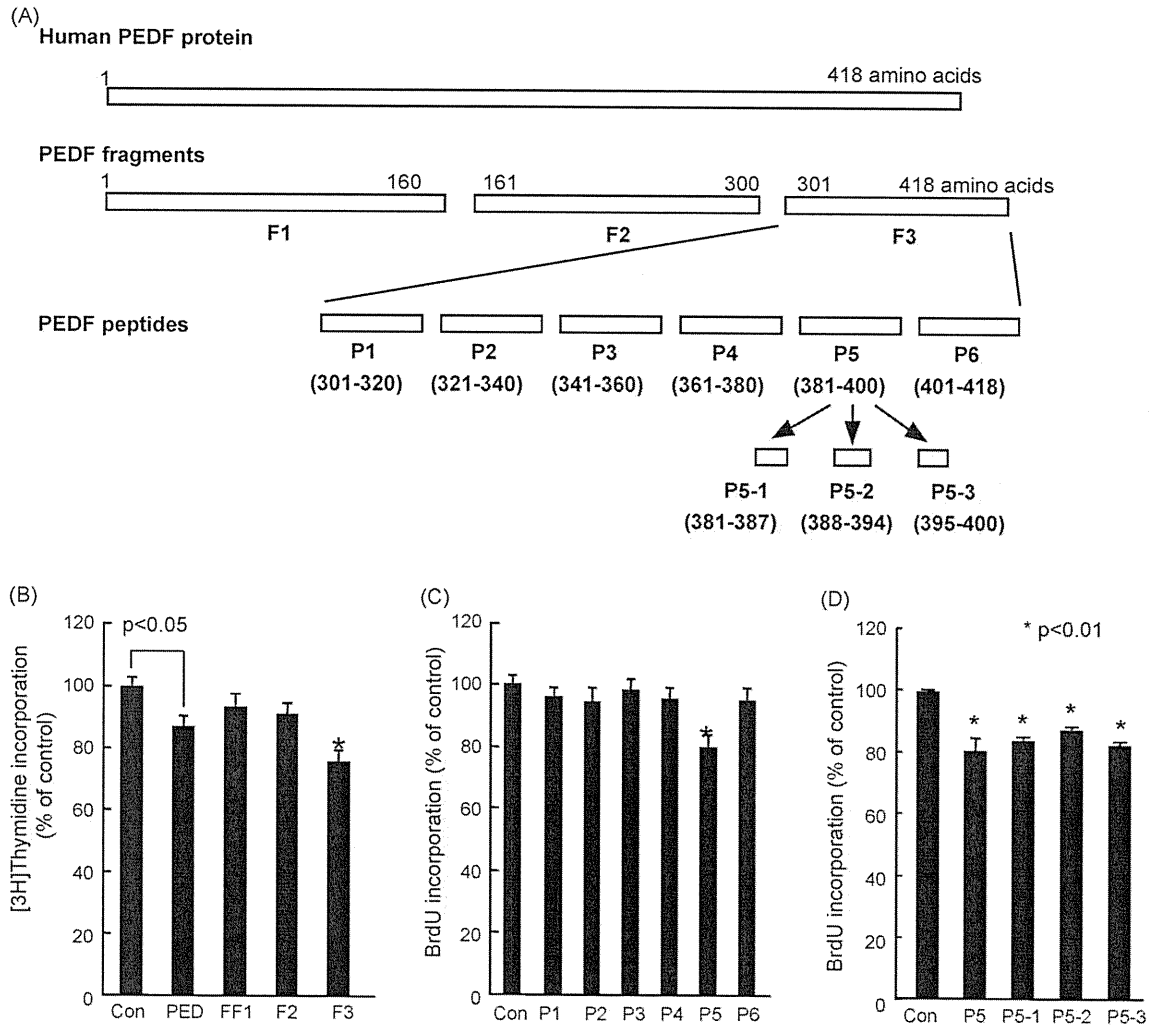

Fig. 5. Anti-angiogeneic activity of PEDF peptides. Diagram of the PEDF peptides studied for their effect on the growth of MG63 cells (B–D) or HUVEC (E). MG63 cells or HUVEC were treated with or without 100 nM PEDF, fragments or peptides and then [^{3}H]thymidine (B) and BrdU incorporation into the cells (C, D) were measured. The percentage of [^{3}H]thymidine or BrdU incorporation is indicated on the ordinate and related to the value of the control. *$p < 0.01$ compared to the value with 100 nM PEDF protein.